

Sulfate Radical-Based Degradation of Organic Pollutants: A Review on Application of Metal-Organic Frameworks as Catalysts

Madhu Kumari and Mrudula Pulimi*

Cite This: *ACS Omega* 2023, 8, 34262–34280

Read Online

ACCESS |



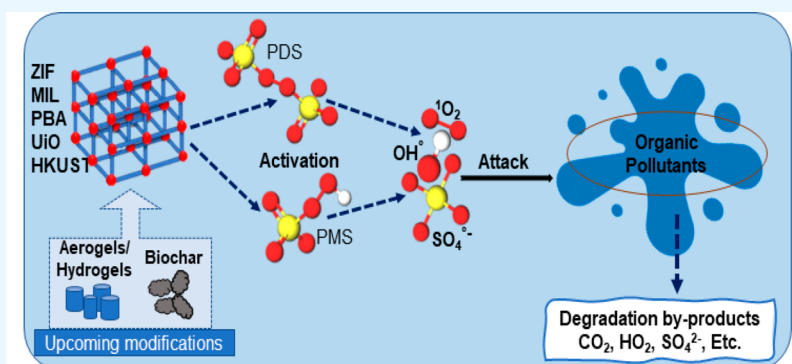
Metrics & More



Article Recommendations



Supporting Information



ABSTRACT: The degradation of organic pollutants present in domestic and industrial effluents is a matter of concern because of their high persistence and ecotoxicity. Recently, advanced oxidation processes (AOPs) are being emphasized for organic pollutant removal from effluents, as they have shown higher degradation efficiencies when compared to conventional activated sludge processes. Sulfate radical-based methods are some of the AOPs, mainly carried out using persulfate (PS) and peroxymonosulfate (PMS), which have gained attention due to the ease of sulfate radical generation and the effective degradation of organic molecules. PMS is gaining more popularity because of its high reactivity and ability to generate excess sulfate radicals. PMS has been the major focus; therefore, its mechanism has been explained, and limitations have been elaborated. The involvement of metal–organic frameworks for PMS/PS activation applied to organic pollutant removal and recent advances in the application of biochar and hydrogel-assisted metal–organic frameworks have been discussed.

1. INTRODUCTION

Our ecosystem has recently been gradually deteriorating due to a wide range of organic pollutants, which are toxic chemicals that adversely affect the health of human beings and the environment around the world. Progressively higher concentrations of organic pollutants sourced from domestic and industrial applications have been observed in the water systems around the world.¹ Organic pollutants are a large class of contaminants which include, to name a few, pesticides, herbicides, insecticides, detergents, endocrine-disrupting chemicals, polycyclic aromatic hydrocarbons, dyes, personal care products, and pharmaceuticals.^{2,3} The increase in the industrial production processes and human activities has resulted in the discharge of organic contaminants into the surroundings, leading to lots of health issues like respiratory ailments, neurological issues, thyroid disorders, etc.⁴ There is an urgent requirement for effective degradation methods for these pollutants. Many treatment methods have been explored to remove and reduce these organic pollutants from the environment. These methods include biodegradation, adsorption, chemical treatments, etc., which have some drawbacks like high energy utilization, limited applications, partial

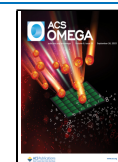
treatment, low efficiency and scalability, secondary contaminants production, etc.^{4,5}

Advanced oxidation processes (AOPs) have been increasingly applied to organic pollutant degradation. Radical-based AOPs are promising environmentally friendly methods with a high oxidation potential that utilize hydroxyl radicals (OH[•]) and sulfate radicals (SO₄^{•-}) for the degradation of organic pollutants.^{6,7} Reactive radicals include the sulfate radicals (SO₄^{•-}), the hydroxyl radicals (HO[•]), superoxide radicals (O₂^{•-}), and hydroperoxyl radicals (OOH[•]).^{7–11} AOPs include different treatment approaches like photocatalysis, the Fenton method, sulfate radical-based oxidation (SR-AOP), ozone-based methods, sonolysis, electrocatalysis, etc.⁸ Combining various AOPs, such as photo-Fenton methods, sono-Fenton,

Received: April 30, 2023

Accepted: August 15, 2023

Published: September 15, 2023



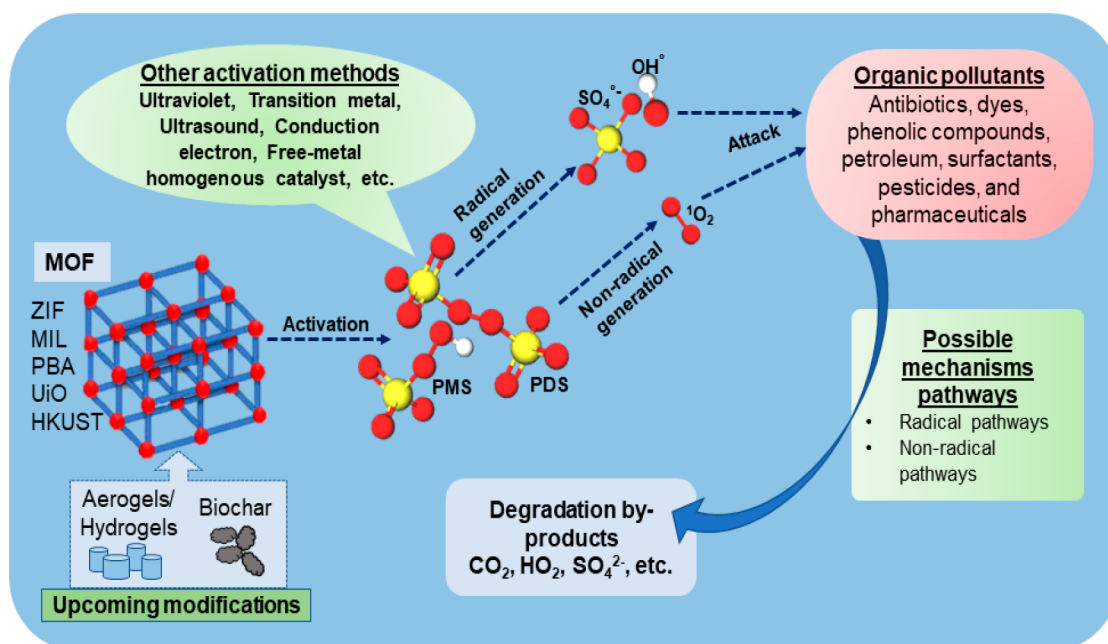


Figure 1. Summary of the mechanisms involved in the adsorption and degradation of pollutants by SR-AOPs

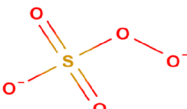

peroxy mono sulfate (PMS)/UV/US, the O_3 /UV process, O_3/H_2O_2 , PMS/ O_3 , etc., has also resulted in effective organic pollutant degradation.⁴ SR-AOPs have gained prominence because of their effectiveness across a wide pH range, higher oxidation potential, and lower dependency on the operational parameters.^{7,12} Persulfate activation, which includes the addition of peroxy monosulfate (PMS) and peroxy disulfate (PDS) as oxidants, is also known as sulfate radical-based oxidation.¹³ As direct interaction with organic pollutants occurs at very low rate, PMS and PDS have to be activated to generate sulfate radicals.¹² Several PMS/PS activation methods have been used, like thermal activation, UV irradiation, alkaline treatment, activated carbon, addition of transition metal ions like Fe(II) and Cu(II), etc.^{9,11} The addition of Fe(II), Co(II), and Cu(II) as activators has been shown to significantly enhance the PMS/PS-based degradation of organic pollutants.^{6,7} Moreover, PS and PMS are relatively inexpensive and sustainable oxidants.^{10,12,14} Compared to PDS, PMS is gaining more attention because of its high reactivity and capacity to oxidize a variety of pollutants.³ Many reviews are available on organic pollutant removal by sulfate oxidation methods.^{10,11,15,16} The findings demonstrate that the removal efficiency of organic pollutants is affected by several factors, including pH, persulfate dose, and reaction time.^{6,11} The main oxidation mechanisms involved are radical-induced oxidation ($SO_4^{\bullet-}$ and OH^{\bullet}), singlet oxygenation (1O_2), electron-mediated transfer, and high-valent-metal-induced oxidation ($\equiv Fe(V)=O$, $\equiv Fe(VI)=O$).¹² The electron-mediated transfer involves the transfer of e^- from electron donors (organics) to electron acceptors (PS/PMS). This method utilizes two electrons from the organic compounds, unlike the radical-based method that utilizes one electron for $SO_4^{\bullet-}$ formation. The presence of metal ions like Fe(II), Ag(II), and Co(II) in their reduced form can lead to other oxidation pathways.¹² Reports are also available on sulfate radical-based oxidation paired with other AOPs, which have enhanced oxidation potential and increase the applicability to degrade a wide range of organic pollutants.^{10,17} Figure 1 summarizes the

mechanisms involved in the degradation of organic pollutants by MOF-based SR-AOPs.

Metal–organic frameworks (MOFs) are a new type of extremely porous and crystalline organic–inorganic hybrid composites created by combining metals and organic linkers. Because of their porous nature, they have been discovered to be quite beneficial as catalysts for PMS/PDS activation.¹⁸ There are numerous benefits of employing MOF-based catalysts over other materials, as MOFs avert homogeneous catalyst leaching by enclosing the cavities or building connections within the framework covalently, as well as the easily modifiable pore size and surface area of the MOFs, due to which they have high specific activity.¹⁹ Several types of MOFs have been reported for PMS/PDS activation, including zeolitic imidazolate frameworks (ZIF),²⁰ Materials Institute Lavoisier (MIL),²¹ University of Oslo-2 (UiO),²² Prussian blue analogues (PBA),²³ Hong Kong University of Science and Technology (HKUST),²⁴ porous coordination network metal–organic framework (PCN-MOF), etc.¹⁸ These MOFs have different metal centers and organic linkers, which can influence their performance in PMS activation.

A few reports are available in literature discussing the PS/PMS activation by MOFs.^{25–29} In a review by Wang et al. from 2022, different MOFs and derived catalysts for PS activation processes were discussed along with the synthesis methods. PS activation methods by MOFs were discussed based on Fenton-like and photo-Fenton methods.²⁵ The effect of the composition and structure of MOF-derived catalysts for PS activation were discussed by Fang et al. 2021, along with the effect of environmental factors and the contribution of different catalytic pathways.²⁶ Du et al. 2021 discussed the preparation methods, characterizations, and mechanisms of action of MOFs.²⁷ Pristine MOFs and MOF derivatives for production of sulfate radicals were summarized by Wang et al. 2019.²⁸ Jiang et al. in 2022 summarized the catalytic activity of MOFs from the perspective of physical activation methods like thermal, photo, and microbial. Additionally, chemical activation by optimization and modification of the MOFs was

Table 1. Properties of PMS/PDS^a

	Peroxymonosulfate	Peroxydisulfate
Molecular configuration		
Abbreviation	PMS	PDS
Molecular Formula	KHSO ₅ • KHSO ₄ • K ₂ SO ₄	K ₂ S ₂ O ₈ / Na ₂ S ₂ O ₈
Bond energy	377 KJ mol ⁻¹	92 KJ mol ⁻¹
Distance of O–O bond structure	1.453 Å	1.497 Å
Water solubility (at 20 °C)	250,000 mgL ⁻¹	730,000 mgL ⁻¹
Standard redox potential	1.82 V	2.12 V
Preferred activation method	Electron-transfer based activation	Energy-transfer based activation

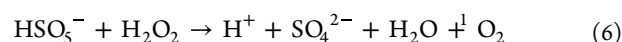
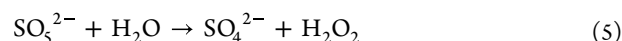
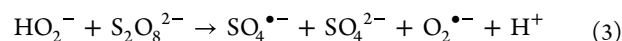
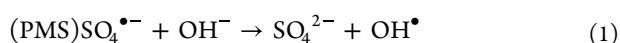
^aAdapted from ref 13. Copyright 2023 Elsevier.

discussed.²⁹ A detailed list of review articles on MOFs as catalysts and PS activators is available in Supporting Information as Table S1.

The objective of this Review is to provide an update on PMS/PDS activation using MOFs as catalysts for organic pollutant degradation. The various types of MOFs based on structure and composition were evaluated for their PS/PMS activation capacities. The roles of metal ion addition and MOF-derived carbonaceous catalysts and other MOF-derived catalysts in PS/PMS activation are summarized. This Review also highlights the emerging MOF derivatives supported by using biochar and aerogels and hydrogels for the activation of sulfate radicals from PS/PMS.

■ PERSULFATE (PMS/PDS) ACTIVATION

The process of converting PMS/PDS into reactive oxygen species (ROS) like radicals of sulfate (SO₄^{•-}), capable of participating in the oxidation of various organic compounds, is referred to as the activation of PMS/PDS.³⁰ This activation can be accomplished in a variety of ways, including the addition of catalysts, pH adjustments, UV light exposure, heat, ultrasound, metal-based catalysts, photoelectron, electricity, etc.¹¹ PMS can be easily activated as compared to PS because of its asymmetrical structure.¹² Therefore, PMS is susceptible to different nucleophiles like CN⁻, N₃⁻, HCO₃⁻, etc. In the presence of halides, PMS gets depleted prior to the oxidation process, which is not observed in the case of PDS.¹² The activation is critical for degradation studies because it increases PS/PMS's ability to generate reactive oxygen species (ROS), which can initiate the degradation process.^{31,32} Another study shows 93.6% of PS decomposition side by side with the pollutant degradation because as the decomposition starts, the radicals are generated, leading to the oxidation process.^{33–35} Table 1 describes the various properties of peroxymonosulfate (PMS) and peroxydisulfate (PDS). The sulfate radical formation reactions involved in the activation process of PMS/PDS are as follows:^{10,36,37}



1.1. Limitations of PMS/PS in Degradation Studies.

There are various limitations of PMS/PS degradation studies, like pH dependency, reactivity with other compounds, the presence of halides, etc.¹²

pH Dependency. Both PMS and PS are pH-dependent, and their oxidation potential decreases when the pH is above 7.0. As a result, in basic environments, the effectiveness of these oxidants may be limited and oxidants like phenol, amine, and sulfide can be used.^{3,14} Additionally, in some cases, the pH below 7.0 leads to a reduction in the oxidation potential of PS/PMS.¹¹ In order to overcome the limitation and increase the reactivity under acidic conditions, PMS and PS can be activated with other oxidants or catalysts like iron, copper, or cobalt.¹¹

Reactivity with Other Compounds. PMS/PS can react with a variety of organic and inorganic compounds present in the water matrices, including humic acids, metals, and chloride ions.¹⁰ This can result in the formation of reactive intermediates and/or a decrease in the overall oxidation efficiency. For example, chloride ions can combine with PMS/PS, resulting in the formation of chlorate, a toxic byproduct.

Environmental Concerns. The use of PMS and PS may also raise environmental concerns due to the potential release of sulfate and other byproducts into the environment.³ The release of sulfate can lead to the formation of sulfuric acid, which can acidify the soil and water and have detrimental effects on the ecosystem.

Lack of Selectivity. PMS and PS are nonselective oxidants that can attack both target and nontarget compounds.¹² This could contribute to the emergence of harmful byproducts and even the destruction of critical analytes. PMS and PS, for

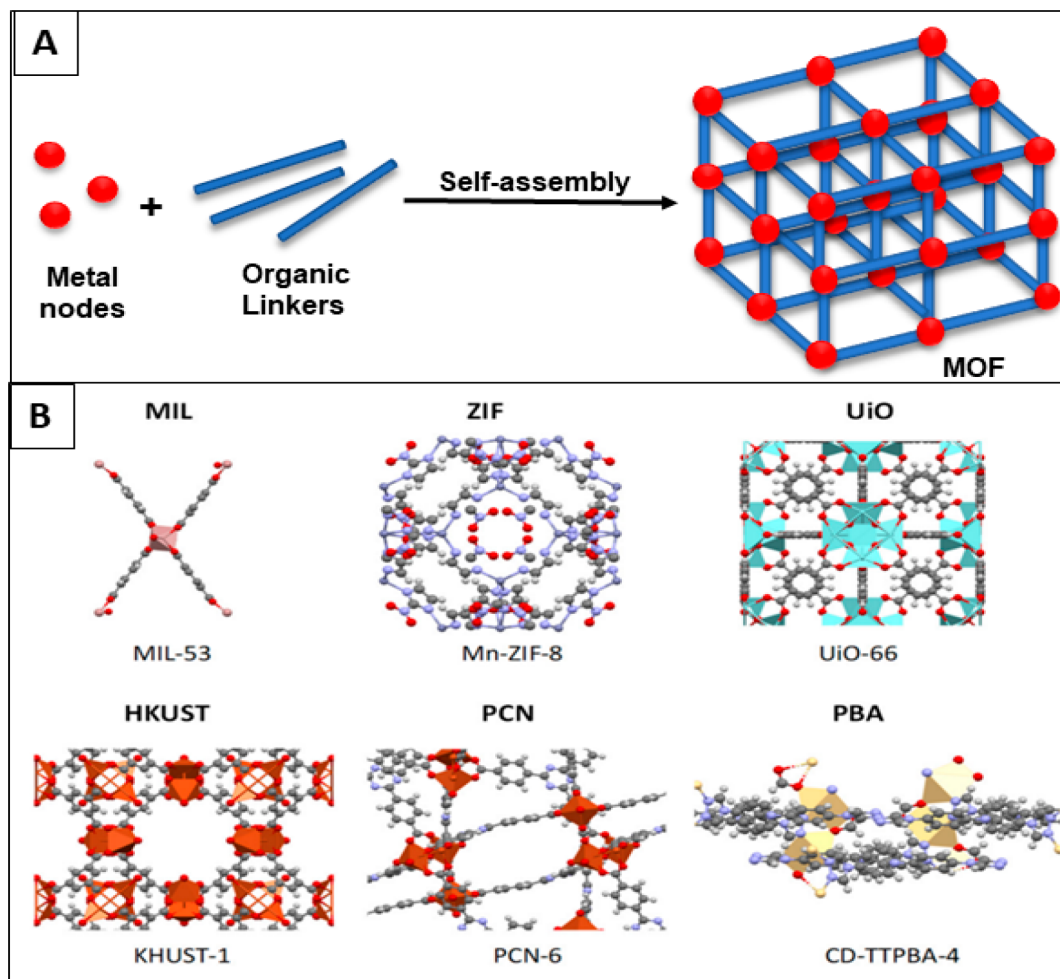


Figure 2. (A) Metal nodes and organic linkers assemble to create MOFs. (B) MOF structures (reproduced from the CSD MOF Collection with license CC-BY-NC-SA 4.0³¹).

example, can degrade natural organic matter in water, resulting in the formation of disinfection byproducts.

Reaction Kinetics. PMS/PS reaction kinetics are highly dependent on experimental conditions such as temperature, pH, and additional substances present. As a result, the optimal conditions for one reaction may not be appropriate for another. Furthermore, the reaction kinetics may be complex and difficult to accurately model, limiting the oxidation process's predictability and reproducibility when applied across different water matrices.

Although PMS and PS are powerful oxidants capable of degrading a variety of contaminants, including pharmaceuticals, dyes, and pesticides, its activation usually requires high temperatures or strong acid conditions. MOF activation provides a promising alternative because they can activate PMS/PS in mild and neutral conditions, which is advantageous for the practical utilization of this technology.⁵

2. COMPARISON OF VARIOUS METHODS OF PS/PMS ACTIVATION WITH MOFS

Various methods involved in the activation of PS/PMS are UV radiation-based, ultrasonication, heat, electrochemical activation, radioactive activation, carbon-based activation, etc. Photobased activation is limited by inefficient penetration of light in real wastewater matrices, which makes it difficult to apply for turbid water matrices, whereas MOFs as activators

can also enhance photocatalytic activity. Similarly, ultrasound-based activation is also restricted by ineffective penetration and is not substrate-specific, unlike MOF-based activation. During the electrochemical activation process of PS/PMS, due to the electrostatic repulsion, PS/PMS does not move toward the cathode surface. Heat activation and electrochemical activation methods are not good for large-scale applications due to the large energy requirements. Transition-metal-based activation methods lead to the problem of metal contamination of water matrices, whereas in the case of MOFs the leaching of the metals is reduced and enhanced reusability of the catalyst has also been observed. Carbon-based catalysts and photoelectron methods exhibit a low mineralization rate that might give incomplete degradation of the pollutant, and the partially degraded intermediates might have higher toxicity. Radioactive activation of PMS raises the concern of radioisotopes and are expensive.

When it comes to activating persulfate or peroxymonosulfate, MOFs offer several advantages over other activators, which are listed below:

- **Enhanced reactivity:** MOFs effectively activate PS/PMS due to their high surface area, promoting interactions, enhancing activator reactivity, and generating reactive radicals.³⁸
- **Tunable catalytic properties:** MOFs can be customized by selecting metal ions and ligands, enhancing catalytic

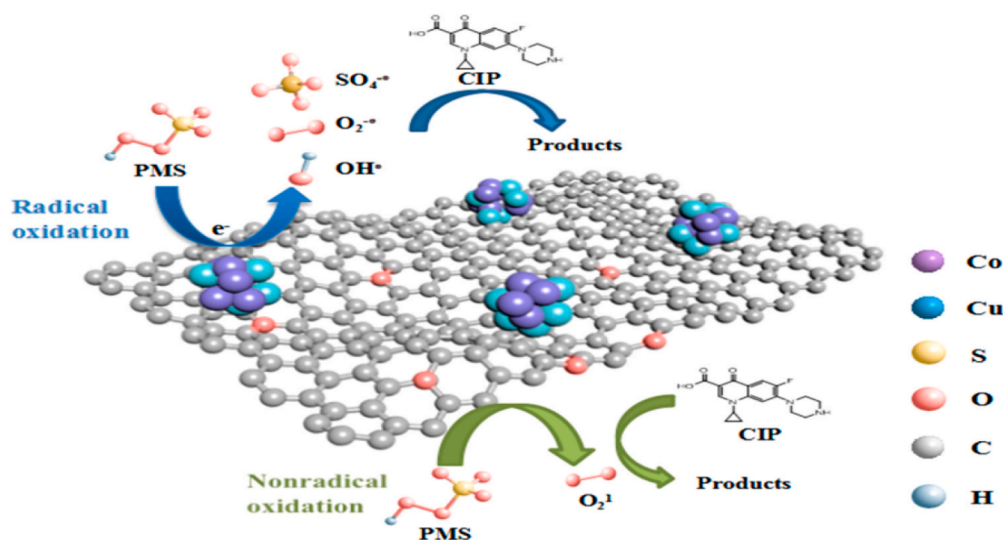


Figure 3. Degradation reaction mechanism via radical and nonradical routes of ciprofloxacin by a CuCo/C + PMS system. Reprinted with permission from ref 144. Copyright 2022 Elsevier.

properties like redox potential, electron transfer capability, and stability for specific reactions or contaminants.^{18,39}

- Facilitated electron transfer: PS/PMS activation involves electron transfer from a catalyst. With MOFs, the presence of redox-active metal centers mediates redox reactions, promoting reactive radical generation and increasing the activation efficiency.^{35,40}

Metal–organic frameworks offer high surface area, tunable catalytic properties, and electron transfer, making them ideal for PS/PMS activation in various applications.

3. METAL–ORGANIC FRAMEWORKS AS CATALYSTS FOR PMS/PS ACTIVATION

MOFs are porous products with a large surface area, changeable pore size, a diverse range of metal centers, and outstanding catalytic characteristics that show great potential as heterogeneous catalyst for PMS/PS activation leading to organic pollutant degradation.^{18,41} MOFs and their composites are widely used as heterogeneous catalysts, photocatalysts, and adsorbents for the removal of toxic pollutants from the environment.^{39,42} They are a form of porous material that is being extensively studied for a variety of applications such as catalysis, storage of gas, and drug delivery because of their flexible properties and huge surface area. Figure 2 shows that MOFs are made up of metal nodes (e.g., chains, atoms, clusters) connected by organic linkers (e.g., carboxylates, phosphonates, and azolates),⁴¹ creating a highly porous stable structure with tunable properties. This tunability allows for optimization of the active sites for PMS/PDS activation. Figure 3B depicts the different types of MOF structures like MIL, ZIF, UiO, HKUST, etc.³¹ The use of MOFs as PMS/PS activation catalysts offers several advantages, including high catalytic activity, selectivity, and reusability.⁴³

A study by Yan et al. in 2022 explains the underlying mechanism involved in the adsorptive removal of pollutants over MOFs, like electrostatic interaction, acid–base interaction, hydrogen-bonding, ion exchange, etc.⁴¹ Degradation of organic pollutants by MOF-based PS/PMS oxidation occurs via radical and nonradical pathways. Radical pathways involve the production $\text{SO}_4^{\bullet-}$ and OH^{\bullet} radicals, whereas the

nonradical pathway involves $^1\text{O}_2$ production.⁴⁴ Various synthesis methods are used for producing the different types of MOF structures, which include the diffusion method, the sonochemical method, the hydro(solvo)thermal method, the microwave method, the electrochemical method, and the mechanochemical method.^{18,43} The synthesis methods have been discussed extensively by Wang et al. in 2022 and Kaur et al. in 2023.^{19,45} The benefits and drawbacks of various synthesis processes are discussed in Table 2.

3.1. Zeolitic Imidazolate Frameworks (ZIF). Zeolitic imidazolate frameworks (ZIF) are created by metal ions (Co,

Table 2. Some Benefits and Drawbacks of Different MOF Synthesis Methods

no.	synthesis method	advantages	disadvantages
1	diffusion method	simple equipment	precursor solubility required
		producing insoluble crystal high yield	long reaction time
2	electrochemical method	mild reaction conditions, fast reaction rate, and low reaction temperature	large-scale synthesis is difficult
		effects of anionic corrosion reduced	products adhere to electrodes easily
		avoids precipitation of metal ions	byproducts produced
3	microwave method	controlled shape and size of products	large-scale synthesis is difficult
		fast reaction time	
		small crystals	
4	mechanochemical method	green process and no organic solvent	formation of defective crystals
		low production cost	
		large scale synthesis and high yield	
5	sonochemical method	simple operation	low purity of products
		energy saving	
		fast reaction rate	
6	hydro- or solvothermal method	high surface area and pore volume	long reaction time
		high thermal stability	toxic organic solvents
		high crystallinity	

Zn, Fe, Cu, etc.) and imidazole derivatives and are topologically structured zeolites.¹⁹ The properties through which the catalytic activity is enhanced are surface sensitivity, large surface area, large pore size, and thermal stability, among others.^{46–49} Furthermore, the unique structural properties of ZIF-MOFs allow for a high degree of control over the catalytic performance, allowing for material tailoring for specific applications.^{36,50,51} There are many different types of ZIFs, which can be classified based on the type of metal ion or cluster used in their construction, the type of organic ligand used, and their pore size and shape.^{52,53} The different types of metal linkers used are 2-nitroimidazole, 2-methylimidazole, benzimidazole, and metronidazole, and the metal oxides are Co_3O_4 , ZnCoO_x , ZnO , and CoS , as mentioned in Table 3.

Table 3. List of Metal Nodes and Linkers of Different Types of ZIF MOFs

no.	ZIF	metal nodes	linker	ref.
01	ZIF-67	Co_3O_4	2-methylimidazole	20
02	ZIF-65	$\text{Zn}(\text{CH}_3\text{COO})_2$	2-nitroimidazole	36
03	ZIF-8	$\text{Co}(\text{NO}_3)_2 \cdot 6\text{H}_2\text{O}$ $\text{Zn}(\text{NO}_3)_2 \cdot 6\text{H}_2\text{O}$	2-methylimidazole	46
04	ZIF-9	$\text{Co}(\text{NO}_3)_2 \cdot 6\text{H}_2\text{O}$	2-methylimidazole	54
05	ZIF-7	ZnO	benzimidazole	55
06	ZIF-78	ZnO	2-nitroimidazole	56
07	ZIF-90	$\text{Zn}(\text{CH}_3\text{COOH})_2 \cdot 2\text{H}_2\text{O}$	imidazolate-2-carboxyaldehyde	57
08	ZIF-71	ZnO	4,5-dichloroimidazole	58
09	ZIF-62	ZnO , $\text{ZnC}_4\text{H}_6\text{O}_4$	5-bromo-1H-benzimidazole	59
10	ZIF-11	$\text{Zn}(\text{CH}_3\text{COOH})_2 \cdot 2\text{H}_2\text{O}$	benzimidazole	60
11	ZIF-12	$\text{Co}(\text{CH}_3\text{COO})_2 \cdot 4\text{H}_2\text{O}$	benzimidazole	60
12	ZIF-100	$\text{C}_2\text{F}_6\text{O}_6\text{S}_2\text{Zn}$	5-chlorobenzimidazole	61
13	ZIF-60	$\text{Zn}(\text{NO}_3)_2 \cdot 6\text{H}_2\text{O}$	imidazole and 2-methylimidazole	62
14	ZIF-L	$\text{Zn}(\text{NO}_3)_2 \cdot 6\text{H}_2\text{O}$	2-methylimidazole	63

When ZIFs are used as pollutant-degrading catalysts, the pollutants are typically adsorbed onto the ZIFs' surfaces.^{51,52} A variety of chemical dynamics, including van der Waals forces, hydrogen bonds, and electrostatic forces, might mediate this adsorption process.^{36,20}

ZIF-67, which includes the Co ion, is the most widely used ZIF for PMS activation. The Co ion plays a critical role in the activation of PMS, where Co^{2+} reacts with HSO_5^- to generate $\text{SO}_4^{\bullet-}$ radicals and Co^{2+} turns to Co^{3+} . Because $\text{SO}_4^{\bullet-}$ radicals are strong oxidizing species that can effectively degrade organic pollutants, Co^{2+} reacting with PMS will be more effective than Co^{3+} .⁵⁰ Because of the higher surface area, better synergistic effect, and porosity, Co ions in ZIF have more activation potential for PMS than free Co_3O_4 nanoparticles.⁵⁰ Pristine ZIF has the disadvantage of leaching of metal ions; therefore, it is important to modify the MOFs to prevent leaching.⁴⁷ Modification of a pristine ZIF leads to enhanced surface area and porosity of the catalysts. Metal leaching gets reduced, which solves the problem of a secondary pollutant.^{50,64} Addition of Co in the form of CoP/CoO_x to ZIF-67 led to a higher PMS activity potential for the degradation of tetracycline. Here also the CoP/CoO_x embedded in the ZIF shows higher activation and lower amount of Co leaching than CoP_x and Co_3O_4 nanoparticles.⁶⁵

Membrane-based ZIFs are extensively used, like ZIF-67@polypropylene membrane, ZIF-67@Resin, ZIF-67/PAN, etc., because of their stable chemical and physical properties and large surface area. A zinc-based ZIF and polyacrylonitrile composite electrospun fibrous membrane (Zn-ZIF-65/PAN) as a PMS activator showed 89.2% (60 min) ciprofloxacin degradation and 55% degradation in five recycling tests. Retreatment of the ZIF/PAN catalyst enhanced the catalytic performance, indicating the renewable property of the catalyst toward PMS.³⁶ In a recent study, when $\text{CoAl}_2\text{O}_4@ \gamma\text{-Al}_2\text{O}_3$ derived from ZIF-67 was used for PMS activation, it was observed that with every successive cycle the degradation efficiency decreased. However, as the catalyst was washed before the fourth cycle with DI water, dried, and cleaned in PMS solution, complete degradation of metronidazole was observed in the fourth cycle within 1 h.²⁰ Further, an aluminum-cobalt layered double hydroxide (AlCo-LDH) catalyst exhibited better catalytic performance with PMS when compared to the pristine Co-ZIF because of the presence of Al ions, which decreases the Co ion requirement for the PMS activation and reducing the effect of Co leaching into the surroundings, which is harmful to the environment.⁴⁸ Modified AlCo-LDH prepared from Co-ZIF provides a larger surface area and pore size when compared Co-ZIF.⁴⁸

The pH of the surroundings plays an important role in the degradation of organic pollutants by the activation of sulfate radicals. For ciprofloxacin degradation, alkaline pH is effective, potentially due to the conversion of $\text{SO}_4^{\bullet-}$ radicals to $\bullet\text{OH}$ as the oxidation rate increases and self-decomposition of PMS takes place.³⁶ Similarly, tetracycline degradation using a ZIF-Co-carbon nitride/PMS (ZCCN) system was effective in alkaline pH.⁶⁶ Additionally, Co leaching decreases as the pH increases from acidic to neutral.⁶⁶ Alternatively, Al-Co-layered double hydroxide derived from Co-ZIF/PMS exhibited high tetracycline degradation in acidic condition because the acid dissociation constant ($\text{p}K_a$) of HSO_5^- was 9.4, indicating the presence of radicals in acidic conditions.⁴⁸ From the reported data, it can be concluded that the degradation efficiency of an organic pollutant depends on variable factors like pH, temperature, PMS concentration, etc. $\text{Fe}_3\text{O}_4\text{-PVP}@ \text{Co-ZIF-67}$ is a polyvinyl pyrrolidone (PVP)-modified magnetic catalyst that exhibits changes in the degradation ability as the loading ratio of $\text{Fe}_3\text{O}_4\text{-PVP}$ and $\text{Co}(\text{NO}_3)_2 \cdot 6\text{H}_2\text{O}$ is modified. Almost 99.8% degradation of bisphenol F in 60 min was observed when the mass ratio of $\text{Fe}_3\text{O}_4\text{-PVP}$ and $\text{Co}(\text{NO}_3)_2 \cdot 6\text{H}_2\text{O}$ was a 1:1 ratio. The optimal ratio of metal ions and MOF ensures that there is a reduction in the wastage of unsaturated metal sites.⁶⁷

ZIFs' catalytic activity can be increased further by pyrolysis. In some studies, it can be observed that due to the modification in the ZIF structure using pyrolysis, the use of transition metal oxides, and the electrospinning method (ZIF-65/PAN, ZIF-67@ $\gamma\text{-Al}_2\text{O}_3$, etc), leaching of the metals was reduced.^{36,20} Pyrolysis can convert ZIFs into highly active and stable catalytic materials with catalytic activity greater than that of the original ZIFs. Pyrolysis can also create additional active sites within materials, which can improve their catalytic performance even further.^{47,68} Another tailored application of a MOF is the preparation of a zinc and cobalt-based catalyst in the same molar (1:1) ratio with pristine ZIF8 and ZIF-67 as precursors under pyrolysis conditions for effective phenol degradation.⁶⁴ After five consecutive repeated cycles, the Co@NC catalyst prepared by pyrolysis by doping nitrogen with

Table 4. Zeolitic Imidazolate Frameworks (ZIF) as PS/PMS Activators for Different Types of Organic Pollutant Degradation

no.	ZIF/catalyst	pollutants	conditions	removal %	references
01	porous carbon (NC) derived from zeolitic imidazolate frameworks-8 (Co NPs) (Co-N@NC-x)	sulfamethoxazole, 20 mg L ⁻¹	catalyst, 0.1 g L ⁻¹ ; PMS, 0.1 g L ⁻¹ ; pH 3.65; T = 25 °C	>96.91% within 90 min	46
02	ZIF-67-derived cobalt/N-doped carbon composites (Co@N-C)	4-chlorophenol	catalyst, 0.05 g L ⁻¹ (or 0.1 g L ⁻¹); PMS, 0.25 mM (or 1 mM PS); pH 7.0	90% in 10 min	53
03	ZIF-67 N-doped porous Co@C nanoboxes (Co@NC)	<i>p</i> -chloroaniline, 0.15 mM	catalyst, 150 mg L ⁻¹ ; PS, 2.5 mM; [Co ²⁺], 0.42 mg L ⁻¹ ; pH 7.5; T = 25 °C	100%	68
04	amorphous CoS _x @SiO ₂ nanocages prepared by sulfurizing ZIF-67@SiO ₂ and thioacetamide (TAA)	sulfamethoxazole, 5 mg L ⁻¹	catalyst, 10 mg; PMS, 0.2 mM	100% within 6 min	69
05	dual zinc-ZIF-8/cobalt-ZIF-67 and derived nanoporous carbons (NPCs)	phenol and <i>p</i> -hydroxybenzoic acid, 20 ppm	catalyst, 0.1 g L ⁻¹ ; PMS, 1 g L ⁻¹ ; T = 25 °C	100% removal of phenol within 10 min	64
06	ZIF procured core-shell Cu ₁ -Co-Zn oxides with Cu _{0.92} Co _{2.08} O ₄ and ZnCo ₂ O ₄ wrapped in carbon (CuCoZnO/C)	phenol, 20 mg L ⁻¹	catalyst, 0.2 g L ⁻¹ ; PMS, 0.2 mM; pH 6.2; T = 25 °C	100% phenol removal in 10 min	51
07	Co-containing carbon (CZIF-67/SiO ₂) obtained by carbonizing yolk-shell ZIFs@SiO ₂ under inert gas	rhodamine, 0.05 g L ⁻¹	catalyst, 0.04 g L ⁻¹ ; PMS, 0.25 g L ⁻¹ ; pH 11; T = 20 °C	100% in 20 min	70
08	hollow carbon shells tridoped with nitrogen, phosphorus, and sulfur from ZIF-67@poly(cyclotriphosphazene-co-4,40-sulfonyl diphenol)	bisphenol A, 25 ppm	catalyst, 0.06 g L ⁻¹ ; PMS, 0.40 g L ⁻¹ ; T = 20 °C	100% in 10 min	71
09	CoAl ₂ O ₄ interfacial from ZIF-67 and Al ₂ O ₃ pellets.	metronidazole, 20 mg L ⁻¹	catalyst, 20 g L ⁻¹ ; PMS, 1.0 mM; pH 6.48; T = 25 °C	97% in 100 min	20
10	hollow Co/NC sheets (HCNSs-9) from pyrolyzing polydopamine coated leaf-like Zn/Co ZIF, ZIFs-L@PDA and ZIFs-NP@PDA	bisphenol F, 20 ppm	catalyst, 0.05 g L ⁻¹ ; PMS, 0.15 g L ⁻¹ ; pH 8.16; T = 35 °C	97–99% in 15 min	72
11	NCNFs (N-doped carbon nanofibers) prepared from cellulose nanofibers (CNFs) and ZIF-8	methylene blue, 10 mg L ⁻¹	catalyst, 0.2 g L ⁻¹ ; PMS, 0.4 g L ⁻¹ ; pH 7.0; T = 25 °C	96% in 15 min, 95% five cycles	73
12	polyoxometalate-derived hierarchical hollow molybdenum/cobalt bimetal oxide nanocages (Mo/Co HHBONs)	levofloxacin, 10 mg L ⁻¹	catalyst, 0.1 g L ⁻¹ ; PMS, 1.0 mM; pH – 7.0	91% in 2 min	74
13	nitrogen-doped porous Co@C nanoboxes (Co@NC) prepared using ZIF-67	<i>p</i> -chloroaniline, 0.15 mM	catalyst, 150 mg L ⁻¹ ; PS, 2.5 mM; pH 7.5; T = 25 °C	99.9% in 60 min	68
14	ZIF-67 supported Cobalt-doped Hollow Carbon Nitride (ZCCN) catalyst	tetracycline, 10 mg L ⁻¹	catalyst, 0.2 g L ⁻¹ ; PMS, 1 mM; pH 7.0; T = 20 °C	99% in 40 min, 65% PMS decomposition	66

Table 5. Materials of Institute Lavoisier (MIL) as PS/PMS Activators for Different Types of Organic Pollutant Degradation

no.	MIL/catalyst	pollutants	conditions	removal %	references
01	bimetal–organic framework MIL-53(Fe, Ni)	rhodamine B, 100 mg L ⁻¹	catalyst, 300 mg L ⁻¹ ; PDS, 0.1 mM	93.9% within 180 min	37
b02	RGO/MIL-101(Fe) (reduced graphene oxide)	trichlorophenol, 20 mg L ⁻¹	catalyst, 0.5 g L ⁻¹ ; PS, 20 mM; pH 3.0	92% within 180 min	79
03	MIL-101(Fe)	orange G dye, 15 mg L ⁻¹	catalyst, 0.1 g L ⁻¹ ; PMS, 0.05 mM; pH 3.0	74.0%	75
04	MIL-88A (Fe)/cotton fibres (MC)	oxytetracycline, 10 mg L ⁻¹	catalyst, 2 g L ⁻¹ ; PDS, 1 mM; pH 4.04	97.5%	81
05	MIL-88A(Fe)/cotton fibers (MC)	tetracycline, 10 mg L ⁻¹	catalyst, 2 g L ⁻¹ ; PDS, 1 mM; pH 4.04	95.2%	81
06	MIL-88A(Fe)/cotton fibers (MC)	chlortetracycline, 10 mg L ⁻¹	catalyst, 2 g L ⁻¹ ; PDS, 1 mM; pH 4.04	100.0%	81
07	iron/carbon (Fe _x C) composites derived from MIL-88A	phenol, 20 mg L ⁻¹	catalyst, 0.3 g L ⁻¹ ; PS, 0.3 g L ⁻¹ ; pH 6.1	98.23% in 60 min	76
08	Fe@N-doped graphene (g-C ₃ N ₄) assisting NH ₂ -MIL-53(Fe)	4-aminobenzoic acid ethyl ether	catalyst, 50 mg L ⁻¹ ; PMS, 0.65 mM; pH 7.0	100% in 60 min	82
09	Fe-MIL-101 on nanofibers of polyacrylonitrile (PAN)	bisphenol, 20 mg L ⁻¹	catalyst, 0.4 g L ⁻¹ ; PMS, 0.2 g L ⁻¹ ; pH 7.0	100% in 6 min	83
10	Composites of core–shell Fe ₃ O ₄ @MIL-101 (Fe)	acid orange 7, 25 mg L ⁻¹	catalyst, 1.0 g L ⁻¹ ; PS, 25 mmol L ⁻¹ ; pH 3.58	98.1% in 60 min	84
11	NH ₂ -MIL-101(Fe) quinone-modified MOF	bisphenol, 60 mg L ⁻¹	catalyst, 0.2 g L ⁻¹ ; PS, 10 mmol L ⁻¹ ; pH 5.76; T = 25 °C	97.7% in 180 min	85

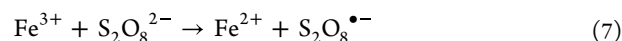
porous Co@C nanoboxes exhibits good stability, with a *p*-chloroaniline degradation rate of 93.9%. In Co@ZIF, the NC demonstrated greater catalytic activity than ZIF-67 alone.⁶⁸ A similar study performed using core–shell copper–cobalt–zinc oxides consisting of Cu_{0.92}Co_{2.08}O₄ and ZnCo₂O₄ derived from ZIF-8 (CuCoZnO/C) showed 60% phenol degradation after the tenth successive cycle, implying the blockage of the reactive sites with the pollutants or intermediates.⁵¹

Further, the combination of PMS/PDS, utilizing ZIF and sonolysis, offers a powerful method for the effective degradation of pollutants. In a study, a combination of ZIF-8 nanomaterials and sonolysis was used for PDS activation and acid orange dye degradation.⁵² In a study, ZIF-67/PMS system shows effective rhodamine B degradation in the presence of UV irradiation and ultrasonication, as it helps in the activation of PMS and generating an excessive amount of free radicals.⁵⁰ Various species like H₂O₂, S₂O₈²⁻, and HSO₅⁻ intervene, generating OH• and SO₄^{•-} radicals and leading to the increased degradation efficiency of the dye. Integration of sonolysis with MOF-activated PDS increases the final performance of the process synergistically and reduced the overall ecotoxicity of Acid Blue 7.⁵² Extensive research has been conducted to evaluate the usage of ZIF-MOFs as PMS/PS precursors in degradation experiments, and a summary of them have been listed in Table 4

3.2. Materials Institute Lavoisier (MIL). MIL-MOFs are formed by mixing metal ions (Cr, Fe, Al, Ti, and V) or transition metal oxides (TiO₂, V₂O₅, Cr₂O₃, and Fe₃O₄) and an organic molecule with two carboxylic groups, which is used as linker. Typical organic linkers used are galacturonic acid, succinic acid, fumaric acid, and terephthalic acid. MIL-MOFs have a specific crystal structure known as the face-centered cubic (fcc) topology. This structure is characterized by a repeating unit cell consisting of a cube-shaped cage formed by 12 metal ions and 8 organic ligands. The cubes are linked together by additional metal ions and ligands to form a three-dimensional porous network. Most of the MILs have an octahedral nanocrystal shape within a range of 100–800 nm.^{75,76} The specific composition, size of the metal ions, and organic ligands used in MILs can be tailored to achieve specific characteristics, like larger specific surface area, large pores, chemical stability, etc. Various research performed to evaluate

the usage of MIL-MOFs as PMS/PS precursors in degradation experiments are listed in Table 5.

In a study, iron based MIL-88A acting as a heterogeneous catalyst for PS activation was synthesized using Fe₂O₃ and fumaric acid in deionized water and exhibited a crystalline hexagonal rod shape morphology with a size range of 100–800 nm.⁷⁷ The Fe³⁺ ions from Fe₂O₃ induce the formation of sulfate radicals, leading to the decolorization of rhodamine B dye (eq 7).⁷⁷ Rhodamine B degradation used MIL-53(Fe, Ni), having a spindle structure and an average diameter of 2.2 nm with a high surface area facilitating the adsorption and dispersion of dye on to the active sites, for the activation of PDS.⁷⁸ Bimetallic organic frames MIL-53(Fe, Ni) are effective for rhodamine B degradation as compared to iron-based MIL-88A.^{77,78} According to Xu et al. (2020), a reduced graphene oxide/MIL-101(Fe) was created as a heterogeneous catalyst that could activate PS for the trichlorophenol degradation by offering a lot of active sites for effective adsorption and conductive RGO.⁷⁹ They discovered that the metal nodes and organic ligands worked together synergistically to activate PMS/PS, resulting in the production of sulfate and hydroxyl radicals.^{37,79}



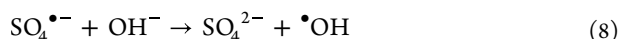
Most of the MIL-88 MOFs are predominantly used in combination with UV irradiation. MIL-88-A in the presence of UV light results in both adsorption and degradation processes, showing the synergistic effects for naproxen degradation.⁸⁰ According to Wang et al. in 2022, the Fe–O bond is important for PDS activation under UV light irradiation, as it demonstrates the effective bonding of MIL-88A(Fe) to cotton fibers (MC). Fixed bed tests reveal that 4.8 L of a tetracycline antibiotics matrix solution can be successfully treated in 24 h and that over 80% of antibiotics can be eliminated after 24 h.⁸¹ The potential mechanism was investigated using active species scavenging studies, which revealed that SO₄^{•-} radicals were the primary active species, with OH• being the secondary main radical in the process.⁸¹ Similarly, under visible-light irradiation, MIL-101(Fe)/g-C₃N₄ composite catalysts exhibiting a uniform octahedral structure are extremely active and durable for activation of PMS for tetracycline hydrochloride

Table 6. University of Oslo (UiO) as PS/PMS Activators for Different Types of Organic Pollutant Degradation

no.	UiO/catalyst	pollutants	conditions	removal %	references
01	magnetic particles with codoped Fe ₃ O ₄ encapsulated in zirconium-based MOFs (Co–Fe ₃ O ₄ @UiO-66)	fenitrothion, 10 mg L ⁻¹	catalyst, 1 g L ⁻¹ ; PMS, 1 mM; T = 25 °C	90.0% in 60 min	91
02	MnO ₂ /UiO-66 composite	oxytetracycline, 50 mg L ⁻¹	catalyst, 50 mg L ⁻¹ ; pH 7.0	79.5% once cycle, 66.2% four cycles	94
03	UiO-66-NH ₂ -ferrocene hybrids with g-C ₃ N ₄ (U–F@CN)	bisphenol-A, 20 mg L ⁻¹	catalyst, 100 mg L ⁻¹ ; PMS, 0.2 g L ⁻¹ ; pH 6.0; T = 25 °C	100% in 60 min	90
04	ZnFe ₂ O ₄ loaded on UiO-66-NH ₂	tetracycline, 25 mg L ⁻¹	catalyst, 20 mg; PS, 3–5 mg	96.2% one cycle, 83.6% five cycles	95
05	UiO-66-NH ₂ with transition metal modification (Fe–UiO-66-NH ₂ , Ni–UiO-66-NH ₂ and Co–UiO-66-NH ₂)	bisphenol A, 20 mg L ⁻¹	catalyst, 10 mg L ⁻¹ ; PMS, 15 mg L ⁻¹ ; pH 6.0; T = 25 °C	97.5 in 60 min (Fe–UiO-66-NH ₂)	96
06	co-anchored single atom on sulfhydryl-decorated UiO-66 (Zr–MSA–Co)	norfloxacin, 20 mg L ⁻¹	catalyst, 0.1 g L ⁻¹ ; PMS, 1.5 mM; pH 6.8; T = 25 °C	99.4% in 240 min	88
07	NH ₂ -UiO-66@BiOI composite photocatalyst with BiOI incorporation	bisphenol A, 10 ppm	catalyst, 10 mg L ⁻¹ ; PMS, 1 mM; pH 6.0; T = 25 °C	99.4% in 12 min 65% mineralization	93
08	Co–UiO-66, cobalt-doped zirconium-based MOF	rhodamine, 30 mg L ⁻¹	catalyst, 10 mg L ⁻¹ ; PMS, 5 mg; pH 6.0; T = 25 °C	97.3% in 45 min	92
09	UiO-66-NH ₂ derivatized with benzothiadiazole modified g-C ₃ N ₄ (UiO-66-NH-BT@g-C ₃ N ₄)	sulfamethoxazole, 10 mg L ⁻¹	catalyst, 5 mg L ⁻¹ ; PS, 30 mg L ⁻¹ ; pH 5.0; T = 25 °C	97.6% one cycle, 91.8% five cycles (80 min)	97
10	UiO-66-NH-BT@g-C ₃ N ₄ -UiO-66-NH ₂ functionalized with benzothiadiazole on carboxyl modified g-C ₃ N ₄	tetracycline, 20 mg L ⁻¹	catalyst, 0.3 g L ⁻¹ ; PMS, 0.4 mM; pH 5.29; T = 25 °C	98.5% in 8 min	89

(TC) degradation. Both radical and nonradical mechanism pathways were involved. The high concentration of active Fe sites and the sizable surface area of the MOF are responsible for MIL-101(Fe) catalytic activity.²¹ It has been concluded that the synergistic effect between g-C₃N₄ and MIL-101(Fe) significantly increases in the presence of light, and the catalyst was structurally stable during the reaction, as the ratio of Fe precursor in the catalyst was same before and after the process.²¹

The PMS decomposition in an acidic environment provides excessive production of SO₄^{•-} radicals and OH[•] radicals formation starts as the pH of the environment increases (eq 8).⁸²



Fe ion leaching was observed to be 0.19 mg L⁻¹ in the MIL-101(Fe)/PMS process, which is nontoxic to the environment.⁷⁵ Fe-MIL-101 on nanofibers of polyacrylonitrile was effectively synthesized, and it was observed that the amount of Fe leaching was 0.13 mg L⁻¹, which is less as compared to various other Fe-based MOF studies.⁸³

3.3. University of Oslo (UiO). A University of Oslo (UiO) MOF is based on a primary building unit made up of linkers (dicarboxylic acid; 1,4-benzenedicarboxylic acid, mercaptosuccinic acid, terephthalic acid, etc.) and metal ions as a secondary building unit (Zr₆(O)₄(OH)₄, ZrCl₄, etc.). The solvothermal approach was used to create UiO-66(Zr) from ZrCl₄ and 1,4-benzenedicarboxylate (BDC), having pore cages that are octahedral and tetrahedral.⁸⁶ The thermodynamic stability of UiO-66 was superior, and the results of the experiments revealed that the framework is durable at pH 14.⁸⁷ It also has qualities like an adequately uniform and large pore size and a predetermined surface area. UiO-2 is a very porous substance with a greater surface area suitable for adsorption and catalytic reactions. At room temperature and neutral pH levels, UiO has been proven to be an excellent catalyst for PS/PMS activation.⁸⁸ The most commonly employed UiO-MOFs in degradation research are UiO-66, UiO-67, UiO-68, and UiO-69, with UiO-66 being the maximum used either directly or with modifications. Most of the UiO-based MOFs exhibit photocatalytic activity, and hence combining photoperoxulfate activation by UiO increases the degradation efficiency.

UiO-66 has been reported to stimulate PMS for the breakdown of variety of pollutants, including bisphenol A (BPA), norfloxacin, and sulfamethoxazole.^{38,89,88,90} Sulfhydryl-decorated UiO-66 embedded with single-atom Co (Zr–MSA–Co) provides Co²⁺ ions that activate PMS to form SO₄^{•-} radicals, which react with norfloxacin, and the remaining sulfate radicals are involved in the formation of OH[•] radicals. The increased activity was attributed by the researchers the significant contact between the S–Co–S active sites and Co being the active center of UiO-66 and PMS, which encouraged the production of sulfate radicals.⁸⁸ This study indicates the elevated degradation efficiency of Zr–MSA–Co/PMS in real water matrices in the presence of Cl⁻ and HCO₃⁻.⁸⁸ In another study, Yin et al. in 2021 synthesized a modified UiO-66 MOF by the interaction with Fe₃O₄ nanoparticles resulting in formation of dual active centers of Fe–Zr.³⁸ In another study, a Co–Fe₃O₄@UiO-66 composite eliminates maximum amount of fenitrothion (FNT) when compared to pristine UiO-66 MOF or PMS. In this case, FNT may be converted to phosphate, leading to secondary pollution, where UiO-66 shows a high affinity by absorbing the released phosphate.⁹¹ PMS activated by a zirconium-based MOF doped with cobalt (Co–UiO-66) was applied to degrade rhodamine B, and both radical and nonradical degradation pathways were observed. The degradation efficiency of catalyst decrease for the fifth successive reuse, potentially due to Co²⁺ leaching, which reduces the active site for the activation of PMS.⁹² In wastewater treatment, various inorganic anions like NO₃⁻ exist that inhibit both the adsorption of the target pollutant and PMS activation.⁸⁷ A BiOI-incorporated NH₂-UiO-66 composite under simulated visible light showed 80% bisphenol A degradation even in the presence of inorganic anions such as Cl⁻, HCO₃⁻, and NO₃⁻. In this method, PMS activation is enhanced by the introduction of various active sites due to the Z-scheme heterojunction. This study also states that excess amount of PMS reacts with the already formed reactive radicals and reduces the effectiveness of the complete process.⁹³ The UV/H₂O₂/PMS–MnO₂/UiO-66 system might be effective in treating oxytetracycline-containing wastewater without prior pH adjustment, indicating the effectiveness of the combined method.⁹⁴ Various studies of UiO-based MOFs as catalysts for

Table 7. Prussian Blue Analogs (PBA) as PS/PMS Activators for Different Types of Organic Pollutant Degradation

no.	PBA	pollutants	conditions	removal%	references
01	Zn–Co Prussian blue analogues	methylene Blue, 100 mg L ⁻¹	catalyst, 0.1 mg L ⁻¹ ; PMS, 1.0 g L ⁻¹ ; pH 6.30; T = 25 °C	100% in 10 min	98
02	Fe–Co PBA/polyacrylonitrile nanofibers	bisphenol A, 20 mg L ⁻¹	catalyst, 233 mg L ⁻¹ ; PMS, 500 mg L ⁻¹ ; pH 2.8; T = 20 °C	67% in 240 min	103
03	PBA with poly(m-phenylenediamine) nanomaterials (PBA@PmPDs) PBA Fe–Co–Co@PmPDs	rhodamine B, 15 mg L ⁻¹	catalyst, 0.1 g L ⁻¹ ; PMS, 0.3 g L ⁻¹ ; T = 25 °C	100% in 60 min	104
04	Fe/Co Prussian blue analogs (PBAs)	bisphenol A, 20 mg L ⁻¹	catalyst, 0.2 g L ⁻¹ ; PMS, 0.2 g L ⁻¹ ; T = 25 °C	96% in 2 min	105
05	Co–Fe PBAs@rGO analogues of Co–Fe Prussian blue (Co–Fe PBAs) with graphene oxide	levofloxacin hydrochloride, 20 mg L ⁻¹	catalyst, 50 mg L ⁻¹ ; PMS, 0.1 g L ⁻¹ ; pH 5.5; T = 20 °C	97.6% in 30 min	107
06	magnetic carbon/cobalt/iron (MCCI) nanocomposite, PBA, cobalt hexacyanoferrate Co ₃ [Fe(CN) ₆] ₂	rhodamine B, 10 mg L ⁻¹	catalyst, 50 mg L ⁻¹ ; PMS, 50 mL ⁻¹ ; T = 30 °C	100%	106
07	iron-based PBAs (Co–Fe PBA, Mn–Fe PBA, Cu–Fe PBA, and Fe–Fe PBA)	<i>p</i> -Nitrophenol, 20 mg L ⁻¹	catalyst, 0.2 g L ⁻¹ ; PMS, 1 g L ⁻¹ ; pH 7.0; T = 30 °C	90% in 60 min	100
08	Mn _{1.8} Fe _{1.2} O ₄ nanospheres	bisphenol A, 10 mg L ⁻¹	catalyst, 0.1 g L ⁻¹ ; PMS, 0.2 g L ⁻¹ ; pH 7.5; T = 25 °C	95% in 30 min	108
09	mesoporous Mn _x Co _{3-x} O ₄ nanocages	carbamazepine - 21.16 μM	catalyst, 50 mg L ⁻¹ ; PMS, 0.5 Mm; pH 6.0; T = 25 °C	100% in 30 min	102
10	NiCo(Fe)-O _x	bisphenol A, 30 mg L ⁻¹	catalyst, 50 mg L ⁻¹ ; PMS, 0.2 g L ⁻¹ ; pH 6.0; T = 25 °C	99.9% in 100 min	109

PMS/PS activation used for the degradation of organic pollutants are listed in Table 6.

3.4. Prussian Blue Analogs (PBA). The formula M₃^(II)[M^(III)(CN)₆]₂ denotes Prussian blue analogs (PBAs) (MII = Co, Cu, Fe, Mn, Ni; MIII = Co, Fe), which are one form of MOF structure made up of cyanide-containing metal sites arranged octahedrally.^{43,23,98,99} During high-temperature pyrolysis, they are directly convertible to porous carbon frameworks while preserving their well-defined surface area (400–450 m² g⁻¹), resulting in a carbonaceous substance having more surface area and interrelated porosities, which helps to improve catalytic performance.⁹⁸ PMS activation by PBA is more smoothly attained due to its distinct internal chemical tunability. Using Prussian blue analogs to produce bimetallic center catalysts for PMS activation is a potential strategy.⁹⁹ However, little is known about how coexisting anions, which are ubiquitous in water matrices, influence the PMS activation by Prussian blue analogs to eliminate pollutants from the environment.^{100,101} In a study, various N-ligand metals were prepared to know the effect of the metal species (Mn–Fe PBA, Co–Fe PBA, Cu–Fe PBA, and Fe–Fe PBA) on *p*-nitrophenol degradation, where pH played an important role in the process of degradation. PMS gets self-decomposed in alkaline conditions by forming SO₅²⁻, which tends to be less reactive; additionally, PMS is more stable under acidic conditions, which makes sulfate radical formation relatively slower.¹⁰⁰ Mn_x(0.5)Co_{3-x}O₄ nanocages prepared using the self-assembly method formed a spindle-like structure and demonstrated catalytic activity, recyclability, and long-term stability over a wide range of pH (5.0–8.0). The catalyst prepared with a surface area of 75.24 m² g⁻¹ and a pore size of 0.206 cm³ g⁻¹ provides higher activation of PMS molecules compared to other PBA MOFs. This study demonstrates that the catalysts (Mn_{0.5}Co_{2.5}O₄) have high catalytic activity and a lower concentration of metal leaching even after five consecutive cycles.¹⁰²

In a study by Wang et al. in 2018, porous nitrogen-doped carbon (PNC) microspheres synthesized using in situ pyrolysis of Zn–Co PBAs act as a catalyst support for PMS activation, which results in more pores, an increased graphitization degree, and an ample amount of nitrogen substitution,

resulting in effective organic pollutant degradation within 10 min. The π -electron of the carbocatalysts cleaves a PMS (–O–O–) bond for the decomposition of pollutants into CO₂, H₂O, and mineralized acids by the action of SO₄^{•-} radicals and OH[•] radicals. Pyrolysis temperature had an evident effect on the catalytic performance of PNC-800. The catalyst prepared at a lower pyrolysis temperature was less effective than the catalyst prepared at a high pyrolysis temperature.⁹⁸ Another study by Wang et al. in 2019 reported that Fe–Co PBA/polyacrylonitrile (FCPBA/PAN) nanofibers with an average size of 800–900 nm were easy to fabricate and can be utilized in industrial sectors, as they provide excellent reusability under acidic pH. The Co²⁺ and Fe²⁺ get oxidized in the presence of HSO₅⁻ to produce SO₄^{•-} radicals, and Co³⁺ and Fe³⁺ react with SO₅⁻ to produce Co²⁺ and Fe²⁺ radicals, respectively, from HSO₅⁻. The leaching of Co ions from FCPBA/PAN was less as compared to Co–Co PBA/PAN after the reaction, indicating the combined effect of Co and Fe can subdue Co leaching.¹⁰³ In a similar study, Fe–Co–Co PBA@poly(m-phenylenediamine) (PmPD) catalysts exhibiting a truncated-cube morphology with 530–730 nm in size were developed and utilized for the effective removal of rhodamine B (RhB) with a lower amount of toxicity to the environment. Co²⁺ and Fe²⁺ activate the PMS once it is transferred from the PmPD shells onto Fe–Co–Co PBA surface, later generating SO₄^{•-} radicals. Co³⁺ and Fe³⁺ reacting with HSO₅⁻ generates SO₅^{•-} radicals which gets converted to SO₄^{•-} radicals and OH[•] radicals reacting with the pollutants and forming degradation products.¹⁰⁴ Core–shell PBA (morphology-polygonal cube) provides a high surface area (576.2 m² g⁻¹) and Fe/Co element ratio (1:1.12), which is higher than the previously mentioned catalysts.¹⁰⁵ Co leaching reduces when the catalyst Fe–Co–Co PBA is coated with PmPDs.^{103,104} Prussian blue analog cobalt hexacyanoferrate Co₃[Fe(CN)₆]₂ used to prepare a magnetic carbon/cobalt/iron (MCCI) nanocomposite having an octahedral structure, which exhibited higher activation of PMS as compared to the Co₃O₄.¹⁰⁶ This study indicates the reduction in the degradation process due to the reduced concentration of PMS. Due to the presence of carbon, cobalt, and cobalt ferrite, MCCI acted as a magnetic heterogeneous catalyst for PMS activation, which can be reused again.¹⁰⁶ A toxicity study was

Table 8. Others MOFs as PS/PMS Activators for Different Types of Organic Pollutant Degradation

no.	MOFs/catalyst	pollutants	conditions	removal %	references
01	Co/CoO/Co ₉ S ₈ @carbon hybrid (Co/CoO/Co ₉ S ₈ @NSOC) with N,S,O doping	sulfamethoxazole, 20 mg L ⁻¹	catalyst, 100 mg L ⁻¹ ; PMS, 0.8 mM; pH 6.0; T = 25 °C	98.78% in 10 min, 90% after 8th cycle	116
02	lanthanum oxide coated with porous carbon derived from MOFs (La-MOF-900)	butylparaben -5 ppm	catalyst, 0.2 g L ⁻¹ ; PS, 1 mM; pH 5.7; T = 25 °C	90%	117
03	lanthanum oxide coated with porous carbon derived from MOFs (La-MOF-900)	arsenite -5 ppm	catalyst, 0.2 g L ⁻¹ ; PS, 1 mM; pH 8.6	80%	117
04	metal-organic framework-2 (MOF-2) nanomaterial (NM) with ultrasound (US)	acid blue, 7-10 mg L ⁻¹	catalyst, 0.6 mg L ⁻¹ ; PS, 6 mmol L ⁻¹ ; pH 5.0; US power, 150 W	76.44% in 60 min	118
05	nitrogen-doped Cu/Fe@PC nanocomposite (Cu/Fe@PC-N)	rhodamine B, 50 mg L ⁻¹	catalyst, 0.1 g L ⁻¹ ; PMS, 0.2 g L ⁻¹ ; pH 4.5	100% in 30 min	32
06	metal-organic bimetallic frameworks (FeCo-BDC)	phenanthrene, 1.0 mg L ⁻¹	catalyst, 50 mg L ⁻¹ ; PMS, 0.6 mM; pH 3.15 T = 25 °C	99.0% in 30 min	119
07	Fe@C composites derived from MOF	sulfamethoxazole, 10 mg L ⁻¹	catalyst, 0.4 g L ⁻¹ ; PS, 0.2 mM; pH Ambient; T = 30 °C	98.3% in 90 min	33
08	Fe ₃ O ₄ @MOF-2 nanocomposite	diazinon, 30 mg L ⁻¹	catalyst, 0.7 g L ⁻¹ ; PS, 10 mmol L ⁻¹ ; pH 3.0; T = 30 °C	98.0% in 120 min, 94.8% 15th cycle	120
09	carbon composites with embedded CoxMn _{3-x} O ₄ nanoparticles (CoxMn _{3-x} O ₄ -C)	bisphenol A, 0.1 mM	catalyst, 0.1 g L ⁻¹ ; PMS, 1.0 mM	100% in 3 min	121
10	Fe(II)-based MOFs	sulfamethoxazole, 0.04 mM	catalyst, 0.5 g L ⁻¹ ; PS, 2 mM; pH Ambient; T = 30 °C	97% in 180 min, 77% PS decomposition	35
11	3D rose-like MoS ₂	tetracycline, 8 mg L ⁻¹	catalyst, 0.3 g L ⁻¹ ; PMS, 1-2 mM; pH 7.0; T = 20 °C	98.9% in 60 min	122
12	bimetallic nitrogen-doped hybrid nanorods (FeCo-NC)	bisphenol A, 50 μM	catalyst, 100 mg L ⁻¹ ; PS, 0.5 mM; pH 7.0; T = 25 °C	100% in 20 min	123
13	Ni-Fe-C-600-acid/GO bimetallic nanocomposite prepared from 2D network of Ni-Fe-MOF and graphene oxide.	p-chloroaniline, 0.15 mM	catalyst, 15 mg L ⁻¹ ; PDS, 0.25 mM; pH 5.0; T = 25 °C	95.4 in 60 min	124

performed on *Vibrio fischeri* by a luminescent bacteria assay, which indicated that PMS was not toxic and that toxicity continuously decreased the concentration of the PMS increased.¹⁰² It is important to analyze the toxicity of the resulting intermediates in a degradation study. PBA MOFs used for PMS activation are listed below in Table 7.

Other Metal-Organic Frameworks. There are various other MOF structures present that are widely used for the efficient removal of organic pollutants by acting as catalysts for PMS/PDS activation, such as HKUST, the combination of MIL and ZIF MOFs, etc. Bimetallic cobalt-zinc MOF (Zn/Co-MOF@rGO-600) has shown PMS activation, resulting in the removal of 91.66% of tetracycline.¹¹⁰ Mn_{0.8}Fe_{2.2}O₄ magnetic nanoparticles in crystal form were effective at degrading bisphenol A and can be regenerated in the open space by 450 °C thermal treatment. Obtained results of this study show that transition metal activation of PMS should be combined with appropriate amounts of Cl⁻ and bicarbonate to ensure extremely effective degradation.¹¹¹ A nickel-cobalt layered double hydroxide (NiCo-LDH) catalyst prepared for PMS activation degraded reactive red 120 dye by 89% in 10 min and 83.6% after five consecutive cycles.¹¹² In a study using bimetallic Fe-Cu organic frameworks (Fe-Cu-MOF@C), complete degradation of 2,4-dichlorophenol was observed in 90 min and good stability was provided after multiple uses; additionally, the catalyst can be regenerated by heat treatment.¹¹³ A study by Liu et al. from 2022 shows that Cu/Fe@PC-derived MOF leads to self-decomposition of PMS by generating singlet oxygen (¹O₂) radicals.³² The high surface area and porosity of HKUST-1 can enhance organic pollutant adsorption, increasing the effectiveness of PMS/PS oxidation.^{24,114}

HKUST impregnated with nickel nitrate catalysts (CuNi@C) revealed a unique PMS activator for acid orange 7 (AO7) oxidative degradation and good reusability. In 60 min, 100% degradation of 0.675 mmol L⁻¹ AO7 was observed but was

negligible when PMS was applied alone. Cu²⁺ and Ni²⁺ synergistically uncover the activation sites on the CuNi@C catalyst activating PMS, leading to formation of SO₄^{•-} radicals.¹¹⁴ The mechanism of PMS activation on HKUST-1 involves the generation of Cu(II)-O-O-Cu(II) species, which can activate PMS effectively and generate sulfate radicals for tetracycline degradation. Addition of g-C₃N₄ to CuMOF lowers the emission peak compared to simple g-C₃N₄. As the amount of CuMOF increases, the photocatalytic PMS activation increases. In the presence of solar light, the g-C₃N₄/CuMOF electrons react with PMS to form SO₄^{•-} radicals. Cu(II) reduces to Cu(I) in the presence of PMS, generating SO₄^{•-} radicals, OH[•] radicals, protons, and O₂^{•-} radicals.¹¹⁵ In a study by Zhang et al. from 2020, more than 95% of rhodamine B and methylene blue was degraded within 120 min under visible light using HKUST-1.²⁴ The HKUST-1/PMS/Vis process enhances photolysis because of the selection of PMS as an electron acceptor. PMS also undergoes self-decomposition by obtaining photoelectrons from HKUST-1 and generates SO₄^{•-} radicals and OH[•] radicals. Free radical generation is confirmed by quenchers exhibiting scavenging activities. In the degradation process of rhodamine B (RhB) by HKUST-1/PMS/Vis, the presence of radical scavenger ethanol inhibited RhB, and tertiary butanol did not show inhibitory effect, which confirms the major oxidizing free radical as SO₄^{•-}.²⁴ Several research studies that have been conducted to evaluate the usage of different types of MOFs as PMS/PS precursors in degradation experiments are listed in Table 8.

4. PEROXYMONOSULFATE/PERSULFATE ACTIVATION USING BIOCHAR-BASED MOFS

Biochar and hydrochar in combination with MOFs have demonstrated significant potential for activating PMS/PS in the elimination of organic contaminants from the aqueous matrices.^{39,125} Biochar is a carbon-rich substance produced by the pyrolysis of organic waste that contains more oxygenated

Table 9. Biochar-Based MOFs as Catalysts for PMS/PDS Activators for Different Types of Organic Pollutant Degradation

no.	MOF	biochar/hydrochar	conditions	removal %	references
01	BC/CoNC biochar composite catalyst derived from ZIF-67 and peanut shell	peanut shell	ciprofloxacin, 20 mg L ⁻¹ ; PMS, 1 mM; Catalyst -0.2 g L ⁻¹ ; pH 5.7	95.9% within 30 min	127
02	ZIF-67-containing lotus leaf biochar substrate (LLZ)	lotus leaf	levofloxacin, 5 mg L ⁻¹ ; PMS, 150 mg mL ⁻¹ ; pH = 6.4; T = 22 °C	99.2% within 16 min	126
03	Co@NPC-CMB-x, Co@ZIF reinforced cow manure biochar (CMB)-		carbamazepine, 15 mg L ⁻¹ ; catalyst, 50 mg L ⁻¹ ; PMS, 0.4 mM; pH 6.8; T = 25 °C	100% in 10 min	128
04	Cobalt nanoparticles composite (Co@N-BC)	ginkgo leaves biochar	doxycycline, 50 mg L ⁻¹ ; catalyst, 0.4 g L ⁻¹ ; PS, 0.4 mM; Without pH adjustment	92.72% in 30 min	40
05	Co ₃ O ₄ /C mounted biochar (Co ₃ O ₄ /C-BC) with ZIF-67	<i>Eichhornia crassipes</i>	bisphenol A, 20 mg L ⁻¹ ; catalyst, 0.3 g L ⁻¹ ; PMS, 1.0 mmol L ⁻¹ ; pH 7.0; T = 30 °C	100% in less than 30 min, 92% after six cycles	133
06	Fe-MOF-CC@MoS ₂ bimetal composite corncob biochar catalyst	corn cob	ciprofloxacin, 20 mg L ⁻¹ ; catalyst, 0.1 g L ⁻¹ ; PMS, 10.1 g L ⁻¹ ; pH 6.5	92.30%, 76.5% after five cycles	134
07	Fe-MOF-CC@MoS ₂ bimetal composite corncob biochar catalyst	corn cob	tetracycline hydrochloride, 20 mg L ⁻¹ ; catalyst, 0.1 g L ⁻¹ ; PMS, 10.1 g L ⁻¹ ; pH 6.5	96.51%	134
08	Fe-MOF-CC@MoS ₂ bimetal composite corncob biochar catalyst	corn cob	nitrofurantoin, 20 mg L ⁻¹ ; catalyst, 0.1 g L ⁻¹ ; PMS, 10.1 g L ⁻¹ ; pH 6.5	88.96%	134
09	Fe-MOF-CC@MoS ₂ bimetal composite corncob biochar catalyst	corn cob	sulfamethoxazole, 20 mg L ⁻¹ ; catalyst, 0.1 g L ⁻¹ ; PMS, 10.1 g L ⁻¹ ; pH 6.5	80.76%	134
10	MOF-Co precursors, ultrafine Co NPs (5 nm) were uniformly embedded into carbonizing rose petals BC (Co@RBC800)	rose petals	levofloxacin, 10 mg L ⁻¹ ; catalyst, 0.2 g L ⁻¹ ; PMS, 0.5 mM; pH = 4.5; T = 25 ± 1 °C	100% in 10 min	129

functional groups and has a higher graphitization degree,⁴⁰ whereas hydrochar is created by hydrothermal carbonization of biomass. Both materials have a porous structure that can be altered further by the addition of metal ions to generate MOFs. Pristine MOFs have low reusability for PMS activation, which can be improved using biochar.¹²⁶

According to Zhang et al. in 2023, ZIF-67 used to derive BC/CoNC derived from ZIF-67 was applied for PMS activation and showed effective ciprofloxacin degradation. When the amount of biochar is high, it provides more active sites of CoNC. The biochar provides uniform transportation and expansion of CoNC by reducing agglomeration and creating space for catalytic action. SO₄^{•-} radicals are produced, which react with water to produce OH[•] radicals. PMS self-decomposition and C=O in the catalyst produce ¹O₂ radicals.¹²⁷ Therefore, as the concentration of the catalyst increases, the rate of removal of the pollutants also increases. In one study, a nitrogen-enriched BC-encapsulated cobalt nanoparticle composite (Co@N-BC) derived from ZIF-67 precursors was produced for PS activation employing a one-step pyrolysis process for the removal of doxycycline, and it demonstrated excellent stability and resistance to inorganic ions. Persulfate (S₂O₈²⁻) gets activated by cobalt nanoparticles and undergoes homolytic cleavage to form SO₄^{•-} radicals, which contribute heavily in the mineralization of doxycycline.⁴⁰ With respect to biochar, the degradation rate is independent of pH, as it shows effective results at varying pH.^{127,128} The temperature used during pyrolysis is critical in the preparation of the catalyst. Biochar prepared at high temperatures (700–1000 °C) provides more active sites by exhibiting higher crystallinity and a higher graphite degree.^{128,129} The degradation mechanism was investigated using quenching studies, electron paramagnetic resonance (EPR) tests, and X-ray photoelectron spectroscopy (XPS) analyses, which revealed that the radical and nonradical routes teamed up leading to the oxidation reaction.^{127,126} Biochar may act like electron mediator accepting e⁻ from PMS (lattice oxygen) and may lead to free e⁻ transfer in between ZIF-67 and biochar, later converting Co(III) to Co(II).¹²⁶

MOFs supported by biochar have several advantages over simple MOFs that make them more effective for certain

applications. First, biochar is a low-cost and renewable resource that is widely available. This means that biochar-based MOFs can be produced at a lower cost, and they are typically synthesized from expensive metal–organic compounds and cost-effective raw waste like lotus leaf, cow manure, etc.^{126,129,128} Second, biochar has a porous structure, which allows for the incorporation of metal ions to form MOFs. The porous structure of biochar provides a high surface area for the metal ions to attach, which enhances the catalytic activity of the MOFs.¹²⁷ According to Lei et al. in 2022, a Co nanoparticles carbon (Co@NPC)–cow manure biochar (CMB)-x biochar-based catalyst was synthesized, and biochar provided excellent catalytic performance of the Co²⁺/PMS system.¹²⁸ In a strong acidic environment with an excess of H⁺ ions in the solution, the O–O bond of the PMS molecule breaks and forms a hydrogen bond, causing radicals to be consumed.¹²⁸ In contrast, simple MOFs have a crystalline structure with well-defined pores that can be restricted in size and distribution. Third, biochar is a carbon-rich material that can act as a reducing agent, improving the MOFs' stability.¹²⁸ The reducing properties of biochar can help to mitigate this degradation and extend the MOFs' lifespan.¹³⁰ Table 9 provides a list of some organic pollutant degradation by activated PMS/PS by biochar-modified MOFs.

Hydrochar-based MOFs for the activation of PMS/PS can be explored, as there are recent studies based on hydrochar-based organic pollutant degradation. The regeneration investigations in a study by Jais et al. in 2021 revealed that the removal of both crystal violet dye and tetracycline was reduced during the first cycle and sustained until the fourth cycle, revealing the solvothermal development of NiFe-MOF on sugar cane baggase hydrochar and producing a stable and recyclable adsorbent. NiFe-MOF@acetylcholine provided a surface area 2.3× and 7× higher as compared to the original biochar and the NiFe-MOF, respectively.¹³¹ Therefore, it can be an effective way to reduce the cost and increase the catalytic oxidation of the catalyst.^{131,132} Hydrochar-based studies need to be performed and analyzed more, as the use of hydrochar can be an efficient method for environmental remediation.

Table 10. MOF-Based PMS Activation Using Aerogels and Hydrogels for Degradation Studies

no.	MOF	AG/HG	condition	removal %	references
01	ZIF-67@cellulose aerogel	cellulose aerogels	<i>p</i> -nitrophenol, 20 mg L ⁻¹ ; catalyst, 600 mg L ⁻¹ ; PMS, 20, 30, and 40 mg (PMS, 600 mg L ⁻¹); pH 6; T = 25 °C	80% within only 20 min	142
02	ZIF-67@cellulose aerogel	cellulose aerogels	tetracycline hydrochloride, 20 mg L ⁻¹ catalyst, 600 mg L ⁻¹ ; PMS, 20, 30, and 40 mg (PMS, 600 mg L ⁻¹); pH 6; T = 25 °C	80% within only 20 min	142
03	cobalt-ZIF@Sugar cane Bagasse Cellulose Aerogels	cellulose aerogels	<i>p</i> -nitrophenol, 10 mg L ⁻¹ ; GEL, 100 mg L ⁻¹ ; PMS, 1 mM; pH 6.8; T = 25 °C	98.5% in 60–70 min	141
04	compressible 3D Fe-doped nitrogen carbon/gelation aerogel (Fe@NC-800/AG)	gelatin aerogels	tetracycline, 30 mg L ⁻¹ ; PMS, 0.3 g L ⁻¹ ; volume, 100 mL	94.3% in 60 min	143
05	cellulose aerogel composite from nanotubes (CoFe _{0.8} @NCNT@CA)	cellulose aerogels	tetracycline, 40 mg L ⁻¹ ; catalyst, 400 mg L ⁻¹ ; PMS, 400 mg L ⁻¹	97.1% in 20 min	140
06	MIL and ZIF doped by Fe/Co and nitrogen with graphene aerogel (C-FeCo, C-CoMIL, C-FeZIF)	graphene aerogels	trichloroacetic acid, 10 mg L ⁻¹ ; PMS, 4 mM; catalyst, 1 g L ⁻¹ ; pH 5.0	81.2% in 160 min	139
07	ZIF-9 and ZIF-12 loaded on cellulose aerogels	cellulose aerogel	<i>p</i> -nitrophenol, 20 mg L ⁻¹ ; PMS, 600 mg L ⁻¹ ; catalyst, 600 mg L ⁻¹ ; pH 6.0; T = 25 °C	90% in 60 min	138
08	ZIF-9 and ZIF-12 loaded on cellulose aerogels	cellulose aerogel	rhodamine B, 50 mg L ⁻¹ ; tetracycline hydrochloride, 30 mg L ⁻¹ ; PMS, 600 mg L ⁻¹ ; catalyst, 600 mg L ⁻¹ ; pH 6.0; T = 25 °C	90% in 60 min	138

5. MOF-BASED PMS ACTIVATION USING AEROGELS

Hydrogels are broadly defined as the hydrated three-dimensional structure of cross-linked networks with a diverse range of structural shapes and chemical compositions containing a significant amount of water.^{135,136} MOFs, on the other hand, can interact with other constituents or modify the characteristics of hydrogel matrices.^{137,138} Aerogels are extremely lightweight nanoporous materials having a continuous 3D nanoporous network structure made up of nanoparticles that have unique structural characteristics like low density, high surface area, and tunable pore volume and high porosity, among others.¹³⁵ The application of MOFs as adsorbents is limited due to their poor stability and difficulty in regeneration. Incorporating MOFs into aerogels/hydrogels can be a potential solution that can improve their stability and allow for easy regeneration.^{138–140} Co-ZIF@sugar cane bagasse aerogels provide Co²⁺, which produced reactive species, and can be recycled, suggesting their wide application for *p*-nitrophenol wastewater treatment.¹⁴¹ Similarly, *p*-nitrophenol was degraded using ZIF-9 and ZIF-12 with cellulose aerogel, where only 90% of the degradation was observed in 1 h.¹³⁸

There are few studies that have explored the use of MOF-based aerogels for organic pollutant degradation. For example, according to Wu et al. in 2022, a catalyst prepared using N-doped C-nanotube/cellulose aerogels derived from a Co–Fe bimetallic MOF (CoFe_{0.8}@NCNT@CA)/PMS system has great stability and regenerability after degrading 97.1% of 40 mg L⁻¹ tetracycline in 20 min. This is because the hydrolysis of PMS generates O₂^{•-} and the cyclic transformation of Co²⁺/Co³⁺ is promoted, which leads to the enhancement of SO₄^{•-} radical formation.¹⁴⁰ In 2020, Wu et al. explained that Co ions of the ZIF-67 composite play an important part in the activation of PMS by the ZIF-67-based cellulose aerogels catalyst for PMS system resulting in tetracycline removal. The aerogel has external spots, a manageable maximum load quantity, and excellent reusability.¹⁴² The 3D compressible iron-doped nitrogen and carbon with gelation aerogel (Fe@NC-800/AG) derived from ZIF-L can be reused ten times, with a tetracycline removal efficiency of up to 90%. Fe⁰/Fe²⁺/Fe³⁺ can produce SO₄^{•-}, SO₄²⁻, SO₅^{•-}, and OH[•] radicals that undergo cyclic transformation, leading to the degradation of tetracycline.¹⁴³ Most of the hydrogel-based MOFs used for PMS/PS activation are ZIF-based, which are listed in Table 10. Therefore, other MOFs need to be explored with aerogels/

hydrogels for PMS/PS activation for organic pollutant degradation.

6. DEGRADATION MECHANISM AND INTERACTION OF MOFS WITH PS/PMS

The mechanism of organic pollutant degradation involves radical and nonradical pathways by activating the PS/PMS using MOF-based catalysts. The radical pathway consists of electron transfers between the MOF-based catalyst and PMS/PS, where the O–O link within the PMS/PS molecule cleaves to yield SO₄^{•-}.²⁶ Depending on the sort of MOF catalyst utilized, there are variable electron transfer factors. For example, if it is a metal-based catalyst, the PMS/PS decomposition will be initiated by the metal centers. For biochar/hydrochar or any other carbon-based catalyst, sp²-hybridized carbon and O₂ functional molecules on the defected portion will lead to the generation of SO₄^{•-} radicals after PMS/PS activation.¹³³ In nonradical pathways, electron transfer takes place between the organic molecules of MOF and PMS/PS, leading to the formation of singlet oxygen.

There are various advantages and disadvantages of these pathways. The radical pathways exhibit better capability to mineralize the pollutants completely because of the oxidizing ability of the free radicals (OH[•] and SO₄^{•-}), but the regeneration of active sites is difficult and selectivity is not satisfactory. In contrast, the nonradical pathway provides high selectivity, high PMS/PS utilization, halide intermediate byproduct reduction, resistance to radical scavengers, inorganic ions and natural organic materials, etc. The disadvantages of the nonradical pathways are the low mineralization capacity, the slow rate of degradation, and the generated radicals with moderate redox potential as compared to OH[•] and SO₄^{•-}. These pathways in MOF-based catalysts are unpredictable and constantly spontaneous, rendering their benefits ineffective. Figure 3 displays ciprofloxacin degradation by Cu@Co-MOF-71-generated CuCo/C-activated PMS via radical and nonradical routes. In this study, 90% of ciprofloxacin was degraded within 30 min at optimum conditions by generating reactive species including SO₄^{•-}, OH[•], and O₂^{•-}, as well as nonradical species such as ¹O₂.¹⁴⁴

The nature of the PS or PMS activation process, as well as the composition and properties of the MOFs, can influence specific interaction mechanisms. Here are some examples of how PS/PMS interact with MOFs:

- Adsorption: MOFs adsorb PS or PMS onto their surfaces due to their high surface area and porosity, allowing activation through interactions with metal centers or organic ligands.⁴⁹
- Electron transfer: MOFs facilitate electron transfer reactions in PS/PMS activation by providing redox-active metal centers, generating reactive species and electrons from PS/PMS molecules.³⁵
- Catalytic reactions: MOFs activate PS/PMS by decomposing metal centers, generating reactive radicals like $\text{SO}_4^{\bullet-}$ that degrade contaminants and enhance activation efficiency.^{18,122}
- Surface reactions: Surface reactions on the MOF material involve activated PS or PMS species reacting with contaminants, causing surface-mediated degradation through electron transfer, radical attack, or oxidative processes.¹²⁷
- Synergistic effects: MOFs and PS/PMS enhance the degradation efficiency by providing additional catalytic sites, stabilizing reactive species, and promoting efficient contaminant degradation through cooperative interactions.^{21,108}
- Selectivity and contaminant removal: MOFs exhibit selectivity in degradation studies, preferring specific contaminants over others, enabling targeted degradation in complex mixtures and removing problematic compounds.

Therefore, the choice of the MOF in degradation studies should be carefully considered to optimize the interaction and enhance the overall degradation performance.

7. CONCLUSION AND FUTURE PROSPECTS

There has been an increase in interest in the advancement of MOF-based catalysts for activation of PMS/PS to degrade the organic pollutants from the environment recently. Therefore, in this Review, we have highlighted the use of metal–organic frameworks as catalysts in the activation of PMS/PDS, which are being used for organic pollutant degradation. Further, moving toward the present research progress, the focus is shifting toward persulfate activation using a MOF combined with biochar-based and hydrogel-based methods due to their environmentally friendly/nontoxic nature. SR-AOPs have shown significant potential to remove organic contaminants from wastewater and water. Further research is needed to optimize the process conditions and investigate the degrading mechanisms of SR-based AOPs for diverse types of organic contaminants. Without any doubt, both PDS and PMS are promising sources of $\text{SO}_4^{\bullet-}$ and OH^{\bullet} radicals. Some future prospects related to the studies are mentioned below:

- Among the extensively accessible hydrochars, MOF-based hydrochars are barely reported for the activation of PMS/PS leading to pollutant degradation. The synergy of MOF and hydrochar may elevate the adsorbent's versatility by creating composites that are porous and have more active sites.
- Fewer studies have been explored on hydrogel and aerogel based MOF studies for PMS/PS activation. Aerogels and hydrogels have been widely used for various applications, such as water treatment, air purification, sensor based studies, etc. But further, these materials with MOFs may be transformed into environmentally friendly substitutes when compared to a

metal-based MOF, which leaches out metals and leaves toxins in the matrix. Compared to MOF and aerogel/hydrogel separately, an aerogel/hydrogel-based MOF might be much more effective in the remediation process of toxic organic pollutants because of the presence of hierarchical tunable porous composition.

- The existing research indicates the increase in the processability, handling, and environmental resistance of the aerogel-based MOFs when compared to other forms of MOFs as catalysts. Hence, these aerogels can be applied in many areas where the simple MOF derivatives/composites are not stable.
- Further research into the activation mechanism and surface-active locations of MOF-derived compounds in PMS/PS activation is required. Sometimes strong oxidants react with the MOF and leads to structural damage, leading to the dissolution of metal nodes and secondary pollutants. Therefore, it is important to assess all the possible conditions while designing the catalyst for PMS/PS activation.
- The degradation pathways cannot be controlled and sometimes both the pathways (radical and nonradical) occur simultaneously, which can be both beneficial and detrimental because the radical pathway gives great mineralization and the nonradical pathway has high selectivity and high PMS/PS utilization. Therefore, before preparing MOFs or MOF-based catalysts, a researcher needs to understand the conversion and balance with respect to these two pathways.
- Extensive study on the nonradical pathway reaction mechanism needs to be explored more.
- Further application of these catalysts for the degradation of other emerging pollutants, such as endocrine-disrupting chemicals, pharmaceutical products, perfluorinated compounds, etc., and the degradation of mixtures of these pollutants could be evaluated.
- Limited research on toxicity studies of pollutants and their byproducts was observed and requires further investigation to assess health risks and safety implications of the treated water. Further toxicity studies can provide a more nuanced understanding of effects and exposure thresholds, aiding informed decision making and environmental protection.

■ ASSOCIATED CONTENT

SI Supporting Information

The Supporting Information is available free of charge at <https://pubs.acs.org/doi/10.1021/acsomega.3c02977>.

List of reviews on similar topics and publication details on the same (PDF)

■ AUTHOR INFORMATION

Corresponding Author

Mrudula Pulimi – Centre for Nanobiotechnology, Vellore Institute of Technology, Vellore, Tamil Nadu 632014, India; orcid.org/0000-0003-1564-3626; Email: pmrudula@vit.ac.in

Author

Madhu Kumari – Centre for Nanobiotechnology, Vellore Institute of Technology, Vellore, Tamil Nadu 632014, India

Complete contact information is available at:

<https://pubs.acs.org/10.1021/acsomega.3c02977>

Notes

The authors declare no competing financial interest.

ACKNOWLEDGMENTS

We would like to thank Vellore Institute of Technology for providing all the facilities.

REFERENCES

- (1) Ahmed, I.; Mondol, M. M. H.; Lee, H. J.; Jhung, S. H. Application of Metal-Organic Frameworks in Adsorptive Removal of Organic Contaminants from Water, Fuel and Air. *Chem. Asian J.* **2021**, *16* (3), 185–196.
- (2) Chalasani, R.; Vasudevan, S. Cyclodextrin-Functionalized Fe₃O₄@TiO₂: Reusable, Magnetic Nanoparticles for Photocatalytic Degradation of Endocrine-Disrupting Chemicals in Water Supplies. *ACS Nano* **2013**, *7* (5), 4093–4104.
- (3) Ghanbari, F.; Moradi, M. Application of Peroxymonosulfate and Its Activation Methods for Degradation of Environmental Organic Pollutants: Review. *Chemical Engineering Journal* **2017**, *310*, 41–62.
- (4) Anjali, R.; Shanthakumar, S. Insights on the Current Status of Occurrence and Removal of Antibiotics in Wastewater by Advanced Oxidation Processes. *J. Environ. Manage* **2019**, *246*, 51–62.
- (5) Rojas, S.; Horcajada, P. Metal-Organic Frameworks for the Removal of Emerging Organic Contaminants in Water. *Chem. Rev.* **2020**, *120* (16), 8378–8415.
- (6) Wang, J.; Wang, S. Activation of Persulfate (PS) and Peroxymonosulfate (PMS) and Application for the Degradation of Emerging Contaminants. *Chem. Eng. J.* **2018**, *334*, 1502–1517.
- (7) Oh, W. D.; Dong, Z.; Lim, T. T. Generation of Sulfate Radical through Heterogeneous Catalysis for Organic Contaminants Removal: Current Development, Challenges and Prospects. *Appl. Catal., B* **2016**, *194*, 169–201.
- (8) Tušar, N. N.; Maučec, D.; Rangus, M.; Arčon, I.; Mazaj, M.; Cotman, M.; Pintar, A.; Kaučič, V. Manganese Functionalized Silicate Nanoparticles as a Fenton-Type Catalyst for Water Purification by Advanced Oxidation Processes (AOP). *Adv. Funct. Mater.* **2012**, *22* (4), 820–826.
- (9) Yang, X. J.; Xu, X. M.; Xu, J.; Han, Y. F. Iron Oxochloride (FeOCl): An Efficient Fenton-like Catalyst for Producing Hydroxyl Radicals in Degradation of Organic Contaminants. *J. Am. Chem. Soc.* **2013**, *135* (43), 16058–16061.
- (10) Wang, J.; Wang, S. Reactive Species in Advanced Oxidation Processes: Formation, Identification and Reaction Mechanism. *Chemical Engineering Journal* **2020**, *401* (June), 126158.
- (11) Guerra-Rodríguez, S.; Rodríguez, E.; Singh, D. N.; Rodríguez-Chueca, J. Assessment of Sulfate Radical-Based Advanced Oxidation Processes for Water and Wastewater Treatment: A Review. *Water (Switzerland)* **2018**, *10* (12), 1828.
- (12) Lee, J.; Von Gunten, U.; Kim, J. H. Persulfate-Based Advanced Oxidation: Critical Assessment of Opportunities and Roadblocks. *Environ. Sci. Technol.* **2020**, *54* (6), 3064–3081.
- (13) Ma, C.; Guo, Y.; Zhang, D.; Wang, Y.; Li, N.; Ma, D.; Ji, Q.; Xu, Z. Metal-Nitrogen-Carbon Catalysts for Peroxymonosulfate Activation to Degrade Aquatic Organic Contaminants: Rational Design, Size-Effect Description, Applications and Mechanisms. *Chemical Engineering Journal* **2023**, *454* (P2), 140216.
- (14) Furman, O. S.; Teel, A. L.; Watts, R. J. Mechanism of Base Activation of Persulfate. *Environ. Sci. Technol.* **2010**, *44* (16), 6423–6428.
- (15) Ghanbari, F.; Moradi, M. Application of Peroxymonosulfate and Its Activation Methods for Degradation of Environmental Organic Pollutants: Review. *Chemical Engineering Journal* **2017**, *310*, 41–62.
- (16) Zheng, X.; Niu, X.; Zhang, D.; Lv, M.; Ye, X.; Ma, J.; Lin, Z.; Fu, M. Metal-Based Catalysts for Persulfate and Peroxymonosulfate Activation in Heterogeneous Ways: A Review. *Chem. Eng. J.* **2022**, *429*, 132323.
- (17) Urán-Duque, L.; Saldarriaga-Molina, J. C.; Rubio-clemente, A. Advanced Oxidation Processes Based on Sulfate Radicals for Wastewater Treatment: Research Trends. *Water* **2021**, *13*, 2445.
- (18) Remya, V. R.; Kurian, M. Synthesis and Catalytic Applications of Metal-Organic Frameworks: A Review on Recent Literature. *Int. Nano Lett.* **2019**, *9* (1), 17–29.
- (19) Kaur, H.; Devi, N.; Siwal, S. S.; Alsanie, W. F.; Thakur, M. K.; Thakur, V. K. Metal-Organic Framework-Based Materials for Wastewater Treatment: Superior Adsorbent Materials for the Removal of Hazardous Pollutants. *ACS Omega* **2023**, *8*, 9004.
- (20) Zhu, M. P.; Yang, J. C. E.; Duan, X.; Zhang, D. D.; Wang, S.; Yuan, B.; Fu, M. L. Interfacial CoAl₂O₄ from ZIF-67@γ-Al₂O₃ Pellets toward Catalytic Activation of Peroxymonosulfate for Metronidazole Removal. *Chemical Engineering Journal* **2020**, *397* (May), 125339.
- (21) Song, J.; Yuan, X.; Sun, M.; Wang, Z.; Cao, G.; Gao, K.; Yang, C.; Zhang, F.; Dang, F.; Wang, W. Oxidation of Tetracycline Hydrochloride with a Photoenhanced MIL-101(Fe)/g-C₃N₄/PMS System: Synergetic Effects and Radical/Nonradical Pathways. *Ecotoxicol. Environ. Saf.* **2023**, *251*, 114524.
- (22) Zhuang, S.; Cheng, R.; Wang, J. Adsorption of Diclofenac from Aqueous Solution Using UiO-66-Type Metal-Organic Frameworks. *Chem. Eng. J.* **2019**, *359*, 354–362.
- (23) Khan, N. A.; Najam, T.; Shah, S. S. A.; Hussain, E.; Ali, H.; Hussain, S.; Shaheen, A.; Ahmad, K.; Ashfaq, M. Development of Mn-PBA on GO Sheets for Adsorptive Removal of Ciprofloxacin from Water: Kinetics, Isothermal, Thermodynamic and Mechanistic Studies. *Mater. Chem. Phys.* **2020**, *245*, 122737.
- (24) Zhang, J.; Su, C.; Xie, X.; Liu, P.; Huq, M. E. Enhanced Visible Light Photocatalytic Degradation of Dyes in Aqueous Solution Activated by HKUST-1: Performance and Mechanism. *RSC Adv.* **2020**, *10* (61), 37028–37034.
- (25) Wang, L.; Luo, D.; Yang, J.; Wang, C. Metal-Organic Frameworks-Derived Catalysts for Contaminant Degradation in Persulfate-Based Advanced Oxidation Processes. *J. Clean. Prod.* **2022**, *375*, 134118.
- (26) Fang, Y.; Yang, Y.; Yang, Z.; Li, H.; Roesky, H. W. Advances in Design of Metal-Organic Frameworks Activating Persulfate for Water Decontamination. *J. Organomet. Chem.* **2021**, *954–955*, 122070.
- (27) Du, X.; Zhou, M. Strategies to Enhance Catalytic Performance of Metal-Organic Frameworks in Sulfate Radical-Based Advanced Oxidation Processes for Organic Pollutants Removal. *Chemical Engineering Journal* **2021**, *403*, 126346.
- (28) Wang, C.; Kim, J.; Malgras, V.; Na, J.; Lin, J.; You, J.; Zhang, M.; Li, J.; Yamauchi, Y. Metal-Organic Frameworks and Their Derived Materials: Emerging Catalysts for a Sulfate Radicals-Based Advanced Oxidation Process in Water Purification. *Small* **2019**, *15* (16), 1900744.
- (29) Jiang, D.; Fang, D.; Zhou, Y.; Wang, Z.; Yang, Z. H.; Zhu, J.; Liu, Z. Strategies for Improving the Catalytic Activity of Metal-Organic Frameworks and Derivatives in SR-AOPs: Facing Emerging Environmental Pollutants. *Environ. Pollut.* **2022**, *306*, 119386.
- (30) Kumari, M.; Pulimi, M. Phthalate Esters: Occurrence, Toxicity, Bioremediation, and Advanced Oxidation Processes. *Water Sci. Technol.* **2023**, *87* (9), 2090–2115.
- (31) Fdez-Sanromán, A.; Rosales, E.; Pazos, M.; Sanroman, A. Metal-Organic Frameworks as Powerful Heterogeneous Catalysts in Advanced Oxidation Processes for Wastewater Treatment. *Applied Sciences (Switzerland)* **2022**, *12* (16), 8240.
- (32) Liu, P.; Zhong, D.; Xu, Y.; Zhong, N. Nitrogen Doped Cu/Fe@PC Derived from Metal Organic Frameworks for Activating Peroxymonosulfate to Degrade Rhodamine B. *J. Environ. Chem. Eng.* **2022**, *10* (3), 107595.
- (33) Pu, M.; Wan, J.; Zhang, F.; Brusseau, M. L.; Ye, D.; Niu, J. Insight into Degradation Mechanism of Sulfamethoxazole by Metal-Organic Framework Derived Novel Magnetic Fe@C Composite Activated Persulfate. *J. Hazard Mater.* **2021**, *414*, 125598.

- (34) Liu, C.; Wang, Y.; Zhang, Y.; Li, R.; Meng, W.; Song, Z.; Qi, F.; Xu, B.; Chu, W.; Yuan, D.; Yu, B. Enhancement of Fe@porous Carbon to Be an Efficient Mediator for Peroxymonosulfate Activation for Oxidation of Organic Contaminants: Incorporation NH₂-Group into Structure of Its MOF Precursor. *Chem. Eng. J.* **2018**, *354*, 835–848.
- (35) Pu, M.; Niu, J.; Brusseau, M. L.; Sun, Y.; Zhou, C.; Deng, S.; Wan, J. Ferrous Metal-Organic Frameworks with Strong Electron-Donating Properties for Persulfate Activation to Effectively Degrade Aqueous Sulfamethoxazole. *Chem. Eng. J.* **2020**, *394*, 125044.
- (36) Pu, M.; Ye, D.; Wan, J.; Xu, B.; Sun, W.; Li, W. Zinc-Based Metal-Organic Framework Nanofibers Membrane ZIF-65/PAN as Efficient Peroxymonosulfate Activator to Degrade Aqueous Ciprofloxacin. *Sep Purif Technol.* **2022**, 299 (May), 121716.
- (37) Zhang, S.; Li, M.; Wang, J.; Zhang, R.; Ma, X.; Tao, H. Bimetal-Organic Framework MIL-53(Fe,Ni) Stimulates Peroxydisulfate to Degrade Rhodamine B: Properties and Degradation Mechanism. *Colloids Surf. A Physicochem Eng. Asp* **2023**, *664*, 131208.
- (38) Yin, Y.; Ren, Y.; Lu, J.; Zhang, W.; Shan, C.; Hua, M.; Lv, L.; Pan, B. Environmental The Nature and Catalytic Reactivity of UiO-66 Supported Fe 3 O 4 Nanoparticles Provide New Insights into Fe-Zr Dual Active Centers in Fenton-like Reactions. *Appl. Catal. B: Environ.* **2021**, *286*, 119943.
- (39) Zhu, L.; Meng, L.; Shi, J.; Li, J.; Zhang, X.; Feng, M. Metal-Organic Frameworks/Carbon-Based Materials for Environmental Remediation: A State-of-the-Art Mini-Review. *J. Environ. Manage* **2019**, *232*, 964–977.
- (40) Jiang, Z.; Wei, J.; Zhang, Y.; Niu, X.; Li, J.; Li, Y.; Pan, G.; Xu, M.; Cui, X.; Cui, N.; Li, J. Electron Transfer Mechanism Mediated Nitrogen-Enriched Biochar Encapsulated Cobalt Nanoparticles Catalyst as an Effective Persulfate Activator for Doxycycline Removal. *J. Clean Prod* **2023**, *384*, 135641.
- (41) Yan, C.; Jin, J.; Wang, J.; Zhang, F.; Tian, Y.; Liu, C.; Zhang, F.; Cao, L.; Zhou, Y.; Han, Q. Metal-Organic Frameworks (MOFs) for the Efficient Removal of Contaminants from Water: Underlying Mechanisms, Recent Advances, Challenges, and Future Prospects. *Coord. Chem. Rev.* **2022**, *468*, 214595.
- (42) Rojas, S.; Horcajada, P. Metal-Organic Frameworks for the Removal of Emerging Organic Contaminants in Water. *Chem. Rev.* **2020**, *120* (16), 8378–8415.
- (43) Xiong, Z.; Jiang, Y.; Wu, Z.; Yao, G.; Lai, B. Synthesis Strategies and Emerging Mechanisms of Metal-Organic Frameworks for Sulfate Radical-Based Advanced Oxidation Process: A Review. *Chemical Engineering Journal* **2021**, *421* (P2), 127863.
- (44) Liu, Y.; Miao, W.; Fang, X.; Tang, Y.; Wu, D.; Mao, S. MOF-Derived Metal-Free N-Doped Porous Carbon Mediated Peroxydisulfate Activation via Radical and Non-Radical Pathways: Role of Graphitic N and C-O. *Chem. Eng. J.* **2020**, *380*, 122584.
- (45) Wang, L.; Luo, D.; Yang, J.; Wang, C. Metal-Organic Frameworks-Derived Catalysts for Contaminant Degradation in Persulfate-Based Advanced Oxidation Processes. *J. Clean Prod* **2022**, *375*, 134118.
- (46) Liu, H.; He, Z.; Li, J.; Zhao, S. Well-Dispersed Cobalt Nanoparticles Encapsulated on ZIF-8-Derived N-Doped Porous Carbon as an Excellent Peroxymonosulfate Activator for Sulfamethoxazole Degradation. *Chemical Engineering Journal* **2023**, *451* (P2), 138597.
- (47) Zhang, X. W.; Lan, M. Y.; Wang, F.; Yi, X. H.; Wang, C. C. ZIF-67-Based Catalysts in Persulfate Advanced Oxidation Processes (PS-AOPs) for Water Remediation. *J. Environ. Chem. Eng.* **2022**, *10* (3), 107997.
- (48) Cao, J.; Sun, S.; Li, X.; Yang, Z.; Xiong, W.; Wu, Y.; Jia, M.; Zhou, Y.; Zhou, C.; Zhang, Y. Efficient Charge Transfer in Aluminum-Cobalt Layered Double Hydroxide Derived from Co-ZIF for Enhanced Catalytic Degradation of Tetracycline through Peroxymonosulfate Activation. *Chem. Eng. J.* **2020**, *382*, 122802.
- (49) Chen, X.; Jiang, X.; Yin, C.; Zhang, B.; Zhang, Q. Facile Fabrication of Hierarchical Porous ZIF-8 for Enhanced Adsorption of Antibiotics. *J. Hazard Mater.* **2019**, *367*, 194–204.
- (50) Lin, K. Y. A.; Chang, H. A. Zeolitic Imidazole Framework-67 (ZIF-67) as a Heterogeneous Catalyst to Activate Peroxymonosulfate for Degradation of Rhodamine B in Water. *J. Taiwan Inst Chem. Eng.* **2015**, *53*, 40–45.
- (51) He, Y.; Wang, Z.; Wang, H.; Almatrafi, E.; Qin, H.; Huang, D.; Zhu, Y.; Zhou, C.; Tian, Q.; Xu, P.; Zeng, G. Confinement of ZIF-Derived Copper-Cobalt-Zinc Oxides in Carbon Framework for Degradation of Organic Pollutants. *J. Hazard Mater.* **2022**, *440* (June), 129811.
- (52) Jamal Sisi, A.; Fathinia, M.; Khataee, A.; Orooji, Y. Systematic Activation of Potassium Peroxydisulfate with ZIF-8 via Sono-Assisted Catalytic Process: Mechanism and Ecotoxicological Analysis. *J. Mol. Liq.* **2020**, *308*, 113018.
- (53) Xue, Y.; Pham, N. N. T.; Nam, G.; Choi, J.; Ahn, Y.; Lee, H.; Jung, J.; Lee, S.; Lee, J. Persulfate Activation by ZIF-67-Derived Cobalt/Nitrogen-Doped Carbon Composites: Kinetics and Mechanisms Dependent on Persulfate Precursor. *Chem. Eng. J.* **2021**, *408*, 127305.
- (54) Zhang, C.; Xiao, Y.; Liu, D.; Yang, Q.; Zhong, C. A Hybrid Zeolitic Imidazolate Framework Membrane by Mixed-Linker Synthesis for Efficient CO₂ Capture. *Chem. Commun.* **2013**, *49* (6), 600–602.
- (55) Li, Y. S.; Liang, F. Y.; Bux, H.; Feldhoff, A.; Yang, W. S.; Caro, J. Molecular Sieve Membrane: Supported Metal-Organic Framework with High Hydrogen Selectivity. *Angewandte Chemie - International Edition* **2010**, *49* (3), 548–551.
- (56) Dong, X.; Huang, K.; Liu, S.; Ren, R.; Jin, W.; Lin, Y. S. Synthesis of Zeolitic Imidazolate Framework-78 Molecular-Sieve Membrane: Defect Formation and Elimination. *J. Mater. Chem.* **2012**, *22* (36), 19222–19227.
- (57) Cao, P.; Cheng, Y.; Li, Z.; Cheng, Y. J.; Chu, X.; Geng, C.; Yin, X.; Li, Y. Intraocular Delivery of ZIF-90-RhB-GW2580 Nanoparticles Prevents the Progression of Photoreceptor Degeneration. *J. Nanobiotechnology* **2023**, *21* (1), 1–17.
- (58) Zhou, T.; Sang, Y.; Wang, X.; Wu, C.; Zeng, D.; Xie, C. Pore Size Dependent Gas-Sensing Selectivity Based on ZnO@ZIF Nanorod Arrays. *Sens Actuators B Chem.* **2018**, *258*, 1099–1106.
- (59) Ma, C.; Li, N.; Xue, W.; Guo, X.; Qiao, Z.; Zhong, C. Polarization Enhanced CH₄/N₂ Separation in Bromine Functionalized ZIF-62 Based Mixed-Matrix Membranes. *J. Membr. Sci.* **2023**, *683* (March), 121829.
- (60) He, M.; Yao, J.; Liu, Q.; Zhong, Z.; Wang, H. Toluene-Assisted Synthesis of RHO-Type Zeolitic Imidazolate Frameworks: Synthesis and Formation Mechanism of ZIF-11 and ZIF-12. *Dalton transactions* **2013**, *42* (42), 16608–16613.
- (61) Wang, N.; Liu, Y.; Qiao, Z.; Diestel, L.; Zhou, J.; Huang, A.; Caro, J. Polydopamine-Based Synthesis of a Zeolite Imidazolate Framework ZIF-100 Membrane with High H₂/CO₂ Selectivity. *J. Mater. Chem. A Mater.* **2015**, *3* (8), 4722–4728.
- (62) Xu, F.; Kou, L.; Jia, J.; Hou, X.; Long, Z.; Wang, S. Metal-Organic Frameworks of Zeolitic Imidazolate Framework-7 and Zeolitic Imidazolate Framework-60 for Fast Mercury and Methylmercury Speciation Analysis. *Anal. Chim. Acta* **2013**, *804*, 240–245.
- (63) Zhang, Y.; Tan, P.; Yang, L.; Zhang, S.; Zhou, B.; Zhang, X.; Huang, H.; Pan, J. Mannitol-Assisted Fe-O Clusters@ZIF-L for Cr(VI) Photocatalytic Reduction under Neutral Conditions Inspired by Fe-Based MOFs Photocatalysts. *Sep Purif Technol.* **2023**, 320 (April), 124174.
- (64) Liang, P.; Wang, Q.; Kang, J.; Tian, W.; Sun, H.; Wang, S. Dual-Metal Zeolitic Imidazolate Frameworks and Their Derived Nanoporous Carbons for Multiple Environmental and Electrochemical Applications. *Chemical Engineering Journal* **2018**, *351* (April), 641–649.
- (65) Liu, Y.; Zou, H.; Ma, H.; Ko, J.; Sun, W.; Andrew Lin, K.; Zhan, S.; Wang, H. Highly Efficient Activation of Peroxymonosulfate by MOF-Derived CoP/CoO x Heterostructured Nanoparticles for the Degradation of Tetracycline. *Chem. Eng. J.* **2022**, *430* (P2), 132816.
- (66) Li, X.; Wang, S.; Xu, B.; Zhang, X.; Xu, Y.; Yu, P.; Sun, Y. MOF Etching-Induced Co-Doped Hollow Carbon Nitride Catalyst for

Efficient Removal of Antibiotic Contaminants by Enhanced Peroxymonosulfate Activation. *Chem. Eng. J.* **2022**, *441* (March), 136074.

(67) Cui, J.; Liu, T.; Zhang, Q.; Wang, T.; Hou, X. Rapid Microwave Synthesis of Fe₃O₄-PVP@ZIF-67 as Highly Effective Peroxymonosulfate Catalyst for Degradation of Bisphenol F and Its Mechanism Analysis. *Chem. Eng. J.* **2021**, *404*, 126453.

(68) Liu, Y.; Chen, X.; Yang, Y.; Feng, Y.; Wu, D.; Mao, S. Activation of Persulfate with Metal-Organic Framework-Derived Nitrogen-Doped Porous Co@C Nanoboxes for Highly Efficient p-Chloroaniline Removal. *Chem. Eng. J.* **2019**, *358*, 408–418.

(69) Wang, F.; Fu, H.; Wang, F. X.; Zhang, X. W.; Wang, P.; Zhao, C.; Wang, C. C. Enhanced Catalytic Sulfamethoxazole Degradation via Peroxymonosulfate Activation over Amorphous CoS_x@SiO₂ Nanocages Derived from ZIF-67. *J. Hazard Mater.* **2022**, *423* (PA), 126998.

(70) Li, X.; Yan, X.; Hu, X.; Feng, R.; Zhou, M. Yolk-Shell ZIFs@SiO₂ and Its Derived Carbon Composite as Robust Catalyst for Peroxymonosulfate Activation. *J. Environ. Manage* **2020**, *262*, 110299.

(71) Ma, W.; Wang, N.; Tong, T.; Zhang, L.; Lin, K. Y. A.; Han, X.; Du, Y. Nitrogen, Phosphorus, and Sulfur Tri-Doped Hollow Carbon Shells Derived from ZIF-67@poly (Cyclotriphosphazene-Co-4, 4'-Sulfonyldiphenol) as a Robust Catalyst of Peroxymonosulfate Activation for Degradation of Bisphenol A. *Carbon N Y* **2018**, *137*, 291–303.

(72) Xiao, C.; Zhang, M.; Wang, C.; Yan, X.; Zhang, H.; Chen, S.; Yao, Y.; Qi, J.; Zhang, S.; Li, J. 2D Metal-Organic Framework Derived Hollow Co/NC Carbon Sheets for Peroxymonosulfate Activation. *Chemical Engineering Journal* **2022**, *444* (March), 136385.

(73) Zhu, W.; Kim, D.; Han, M.; Jang, J.; Choi, H.; Kwon, G.; Jeon, Y.; Yeol Ryu, D.; Lim, S. H.; You, J.; Li, S.; Kim, J. Fibrous Cellulose Nanoarchitectonics on N-Doped Carbon-Based Metal-Free Catalytic Nanofilter for Highly Efficient Advanced Oxidation Process. *Chem. Eng. J.* **2023**, *460*, 141593.

(74) Yang, X.; Xie, X.; Li, S.; Zhang, W.; Zhang, X.; Chai, H.; Huang, Y. The POM@MOF Hybrid Derived Hierarchical Hollow Mo/Co Bimetal Oxides Nanocages for Efficiently Activating Peroxymonosulfate to Degrade Levofloxacin. *J. Hazard Mater.* **2021**, *419* (March), 126360.

(75) Moazeni, M.; Hashemian, S. M.; Sillanpää, M.; Ebrahimi, A.; Kim, K. H. A Heterogeneous Peroxymonosulfate Catalyst Built by Fe-Based Metal-Organic Framework for the Dye Degradation. *J. Environ. Manage* **2022**, *303*, 113897.

(76) Li, X.; Liao, F.; Ye, L.; Yeh, L. Controlled Pyrolysis of MIL-88A to Prepare Iron/Carbon Composites for Synergistic Persulfate Oxidation of Phenol: Catalytic Performance and Mechanism. *J. Hazard Mater.* **2020**, *398* (May), 122938.

(77) Andrew Lin, K.-Y.; Chang, H.-A.; Hsu, C.-J. Iron-Based Metal Organic Framework, MIL-88A, as a Heterogeneous Persulfate Catalyst for Decolorization of Rhodamine B in Water. *RSC Adv.* **2015**, *5*, 32520–32530.

(78) Zhang, S.; Li, M.; Wang, J.; Zhang, R.; Ma, X.; Tao, H. Bimetal-Organic Framework MIL-53(Fe,Ni) Stimulates Peroxydisulfate to Degrade Rhodamine B: Properties and Degradation Mechanism. *Colloids Surf. A Physicochem Eng. Asp* **2023**, *664*, 131208.

(79) Xu, Y.; Wang, Y.; Wan, J.; Ma, Y. Reduced Graphene Oxide-Supported Metal Organic Framework as a Synergistic Catalyst for Enhanced Performance on Persulfate Induced Degradation of Trichlorophenol. *Chemosphere* **2020**, *240*, 124849.

(80) El Asmar, R.; Baalbaki, A.; Abou Khalil, Z.; Naim, S.; Bejjani, A.; Ghauch, A. Iron-Based Metal Organic Framework MIL-88-A for the Degradation of Naproxen in Water through Persulfate Activation. *Chem. Eng. J.* **2021**, *405*, 126701.

(81) Wang, J. S.; Yi, X. H.; Xu, X.; Ji, H.; Alanazi, A. M.; Wang, C. C.; Zhao, C.; Kaneti, Y. V.; Wang, P.; Liu, W.; Yamauchi, Y. Eliminating Tetracycline Antibiotics Matrix via Photoactivated Sulfate Radical-Based Advanced Oxidation Process over the Immobilized MIL-88A: Batch and Continuous Experiments. *Chemical Engineering Journal* **2022**, *431* (P3), 133213.

(82) Liu, C.; Liu, L.; Tian, X.; Wang, Y.; Li, R.; Zhang, Y.; Song, Z.; Xu, B.; Chu, W.; Qi, F.; Ikhlag, A. Coupling Metal-Organic Frameworks and g-C₃N₄ to Derive Fe@N-Doped Graphene-like Carbon for Peroxymonosulfate Activation: Upgrading Framework Stability and Performance. *Appl. Catal., B* **2019**, *255* (April), 117763.

(83) Chen, S.; Li, M.; Zhang, M.; Wang, C.; Luo, R.; Yan, X.; Zhang, H.; Qi, J.; Sun, X.; Li, J. Metal Organic Framework Derived One-Dimensional Porous Fe/N-Doped Carbon Nanofibers with Enhanced Catalytic Performance. *J. Hazard Mater.* **2021**, *416* (April), 126101.

(84) Yue, X.; Guo, W.; Li, X.; Zhou, H.; Wang, R. Core-Shell Fe₃O₄@MIL-101(Fe) Composites as Heterogeneous Catalysts of Persulfate Activation for the Removal of Acid Orange 7. *Environmental Science and Pollution Research* **2016**, *23* (15), 15218–15226.

(85) Li, X.; Guo, W.; Liu, Z.; Wang, R.; Liu, H. Quinone-Modified NH₂-MIL-101(Fe) Composite as a Redox Mediator for Improved Degradation of Bisphenol A. *J. Hazard Mater.* **2017**, *324*, 665–672.

(86) Safaralizadeh, E.; Mahjoub, A. R.; Fazlali, F.; Bagheri, H. Facile Construction of C₃N₄-TE@TiO₂/UiO-66 with Double Z-Scheme Structure as High Performance Photocatalyst for Degradation of Tetracycline. *Ceram. Int.* **2021**, *47* (2), 2374–2387.

(87) Yuan, N.; Gong, X.; Sun, W.; Yu, C. Advanced Applications of Zr-Based MOFs in the Removal of Water Pollutants. *Chemosphere* **2021**, *267*, 128863.

(88) Wang, H.; Wang, C.; Wang, X.; Chen, Q.; Liu, S.; Cai, R.; Haigh, S. J.; Sun, Y.; Yang, D. Journal of Environmental Chemical Engineering Cobalt Atom Sites Anchored on Sulfhydryl Decorated UiO-66 to Activate Peroxymonosulfate for Norfloxacin Degradation. *J. Environ. Chem. Eng.* **2023**, *11* (1), 108972.

(89) Wang, Y.; Liu, C.; Wang, C.; Hu, Q.; Ding, L. Chemosphere 0D/3D NiCo₂O₄/Defected UiO-66 Catalysts for Enhanced Degradation of Tetracycline in Peroxymonosulfate/Simulated Sunlight Systems: Degradation Mechanisms and Pathways. *Chemosphere* **2022**, *299* (March), 134322.

(90) Huang, Z.; Yu, H.; Wang, L.; Liu, X.; Ren, S.; Liu, J. Ferrocene-Modified UiO-66-NH₂ Hybrids with g-C₃N₄ as Enhanced Photocatalysts for Degradation of Bisphenol A under Visible Light. *J. Hazard Mater.* **2022**, *436* (March), 129052.

(91) Zheng, W.; Sun, Y.; Gu, Y. Assembly of UiO-66 onto Co-Doped Fe₃O₄ Nanoparticles to Activate Peroxymonosulfate for Efficient Degradation of Fenitrothion and Simultaneous in-Situ Adsorption of Released Phosphate. *J. Hazard Mater.* **2022**, *436* (March), 129058.

(92) Ma, L.; Feng, X.; Cai, F.; Sun, C.; Ding, H. Colloids and Surfaces A: Physicochemical and Engineering Aspects Cobalt-Doped UiO-66 Nanoparticle as a Photo-Assisted Fenton-like Catalyst for the Degradation of Rhodamine B. *Colloids Surf. A Physicochem Eng. Asp* **2022**, *643* (March), 128734.

(93) Ji, R.; Zhang, Z.; Tian, L.; Jin, L.; Xu, Q.; Lu, J. Z-Scheme Heterojunction of BiOI Nanosheets Grown in Situ on NH₂-UiO-66 Crystals with Rapid Degradation of BPA in Real Water. *Chemical Engineering Journal* **2023**, *453* (P2), 139897.

(94) Zhou, Y.; Feng, S.; Duan, X.; Zheng, W.; Shao, C.; Wu, W.; Jiang, Z.; Lai, W. Journal of Solid State Chemistry MnO₂/UiO-66 Improves the Catalysed Degradation of Oxytetracycline under UV/H₂O₂/PMS System. *J. Solid State Chem.* **2021**, *300* (April), 122231.

(95) Wu, W.; Feng, S.; Zheng, W.; Shao, C.; Jiang, Z. Enhancing Visible-Light Photocatalytic Degradation of Tetracycline by ZnFe₂O₄ Loaded on UiO-66-NH₂ under Activated Persulfate. *Res. Chem. Intermed.* **2021**, *47* (8), 3313–3328.

(96) Lv, S.; Wang, X.; Wei, X.; Zhang, Y.; Cong, Y.; Che, L. Introduction of Cluster-to-Metal Charge Transfer in UiO-66-NH₂ for Enhancing Photocatalytic Degradation of Bisphenol A in the Existence of Peroxymonosulfate. *Sep Purif Technol.* **2022**, *292* (18), 121018.

(97) Lv, S. W.; Liu, J. M.; Li, C. Y.; Zhao, N.; Wang, Z. H.; Wang, S. In Situ Growth of Benzothiadiazole Functionalized UiO-66-NH₂ Carboxyl Modified g-C₃N₄ for Enhanced Photocatalytic Degradation of Sulfamethoxazole under Visible Light. *Catal. Sci. Technol.* **2020**, *10* (14), 4703–4711.

- (98) Wang, N.; Ma, W.; Ren, Z.; Du, Y.; Xu, P.; Han, X. Prussian Blue Analogues Derived Porous Nitrogen-Doped Carbon Microspheres as High-Performance Metal-Free Peroxymonosulfate Activators for Non-Radical-Dominated Degradation of Organic Pollutants. *J. Mater. Chem. A Mater.* **2018**, *6* (3), 884–895.
- (99) Wang, J.; Zhuang, S.; Liu, Y. Metal Hexacyanoferrates-Based Adsorbents for Cesium Removal. *Coord. Chem. Rev.* **2018**, *374*, 430–438.
- (100) Yang, Y.; Gu, Y.; Lin, H.; Jie, B.; Zheng, Z.; Zhang, X. Bicarbonate-Enhanced Iron-Based Prussian Blue Analogs Catalyze the Fenton-like Degradation of p-Nitrophenol. *J. Colloid Interface Sci.* **2022**, *608*, 2884–2895.
- (101) Wang, J.; Wang, S. Effect of Inorganic Anions on the Performance of Advanced Oxidation Processes for Degradation of Organic Contaminants. *Chem. Eng. J.* **2021**, *411*, 128392.
- (102) Deng, J.; Cheng, Y.-q.; Lu, Y.-a.; Crittenden, J. C.; Zhou, S.-q.; Gao, N.-y.; Li, J. Mesoporous Manganese Cobaltite Nanocages as Effective and Reusable Heterogeneous Peroxymonosulfate Activators for Carbamazepine Degradation. *Chem. Eng. J.* **2017**, *330*, 505–517.
- (103) Wang, H.; Wang, C.; Qi, J.; Yan, Y.; Zhang, M.; Yan, X.; Sun, X.; Wang, L.; Li, J. Spiderweb-like Fe-Co Prussian Blue Analogue Nanofibers as Efficient Catalyst for Bisphenol-A Degradation by Activating Peroxymonosulfate. *Nanomaterials* **2019**, *9* (3), 402.
- (104) Zeng, L.; Xiao, L.; Shi, X.; Wei, M.; Cao, J.; Long, Y. Core-Shell Prussian Blue Analogues@ Poly(m-Phenylenediamine) as Efficient Peroxymonosulfate Activators for Degradation of Rhodamine B with Reduced Metal Leaching. *J. Colloid Interface Sci.* **2019**, *534*, 586–594.
- (105) Zhang, W.; Zhang, H.; Yan, X.; Zhang, M.; Luo, R.; Qi, J.; Sun, X.; Shen, J.; Han, W.; Wang, L.; Li, J. Controlled Synthesis of Bimetallic Prussian Blue Analogues to Activate Peroxymonosulfate for Efficient Bisphenol A Degradation. *J. Hazard Mater.* **2020**, *387*, 121701.
- (106) Lin, K. Y. A.; Chen, B. J. Prussian Blue Analogue Derived Magnetic Carbon/Cobalt/Iron Nanocomposite as an Efficient and Recyclable Catalyst for Activation of Peroxymonosulfate. *Chemosphere* **2017**, *166*, 146–156.
- (107) Pi, Y.; Ma, L.; Zhao, P.; Cao, Y.; Gao, H.; Wang, C.; Li, Q.; Dong, S.; Sun, J. Facile Green Synthetic Graphene-Based Co-Fe Prussian Blue Analogues as an Activator of Peroxymonosulfate for the Degradation of Levofloxacin Hydrochloride. *J. Colloid Interface Sci.* **2018**, *526*, 18–27.
- (108) Huang, G. X.; Wang, C. Y.; Yang, C. W.; Guo, P. C.; Yu, H. Q. Degradation of Bisphenol A by Peroxymonosulfate Catalytically Activated with Mn_{1.8}Fe_{1.2}O₄ Nanospheres: Synergism between Mn and Fe. *Environ. Sci. Technol.* **2017**, *51* (21), 12611–12618.
- (109) Ye, J.; Zhuang, G.; Wen, Y.; Wei, J.; Chen, J.; Zhuang, Z.; Yu, Y. Three-Dimensional Zigzag Prussian Blue Analogue and Its Derivates for Bisphenol A Scavenging: Inhomogeneous Spatial Distribution of FeIII in Anisotropic Etching of PBA. *Chem. Eng. J.* **2019**, *372*, 260–268.
- (110) Qi, M.; Lin, P.; Shi, Q.; Bai, H.; Zhang, H.; Zhu, W. A Metal-Organic Framework (MOF) and Graphene Oxide (GO) Based Peroxymonosulfate (PMS) Activator Applied in Pollutant Removal. *Process Safety and Environmental Protection* **2023**, *171*, 847–858.
- (111) Qiu, X.; Yang, S.; Dzakpasu, M.; Li, X.; Ding, D.; Jin, P.; Chen, R.; Zhang, Q.; Wang, X. C. Attenuation of BPA Degradation by SO₄[Rad]⁻ in a System of Peroxymonosulfate Coupled with Mn/Fe MOF-Templated Catalysts and Its Synergism with Cl⁻ and Bicarbonate. *Chemical Engineering Journal* **2019**, *372* (April), 605–615.
- (112) Ramachandran, R.; Sakthivel, T.; Li, M.; Shan, H.; Xu, Z.-X.; Wang, F. Efficient Degradation of Organic Dye Using Ni-MOF Derived NiCo-LDH as Peroxymonosulfate Activator. *Chemosphere* **2021**, *271*, 128509.
- (113) Guo, S.; Ren, D.; Huang, Y.; Wang, Z.; Zhang, S.; Zhang, X.; Gong, X. A Novel Carbonized Derivative of Fe-Cu Bimetallic Organic Framework (Fe-Cu-MOF@C): Preparation and Optimization. *Water Sci. Technol.* **2022**, *86* (10), 2701–2717.
- (114) Huang, X.; Zhang, J.; Zhang, X.; Wu, Q. P.; Yan, C. H. Activation of Peroxymonosulfate by CuNi@C Derived from Metal-Organic Frameworks Precursor. *Aust. J. Chem.* **2018**, *71* (11), 874–881.
- (115) Zhang, Y.; He, K.; Han, N.; Wang, L.; Huang, J.; She, H.; Bai, Y.; Wang, Q. Integration between CuMOF and G-C₃N₄ for Effective Suppressing Charge Recombination in Photocatalytic Peroxymonosulfate Activation. *J. Alloys Compd.* **2023**, *952*, 170008.
- (116) Jiang, Y.; Wang, J.; Liu, B.; Jiang, W.; Zhou, T.; Ma, Y.; Che, G.; Liu, C. Superhydrophilic N,S,O-Doped Co/CoO/Co₉S₈@carbon Derived from Metal-Organic Framework for Activating Peroxymonosulfate to Degrade Sulfamethoxazole: Performance, Mechanism Insight and Large-Scale Application. *Chemical Engineering Journal* **2022**, *446* (P4), 137361.
- (117) Chen, C.; Xu, L.; Huo, J. B.; Gupta, K.; Fu, M. L. Simultaneous Removal of Butylparaben and Arsenite by MOF-Derived Porous Carbon Coated Lanthanum Oxide: Combination of Persulfate Activation and Adsorption. *Chem. Eng. J.* **2020**, *391*, 123552.
- (118) Sisi, A. J.; Khataee, A.; Fathinia, M.; Vahid, B. Ultrasonic-Assisted Degradation of a Triarylmethane Dye Using Combined Peroxydisulfate and MOF-2 Catalyst: Synergistic Effect and Role of Oxidative Species. *J. Mol. Liq.* **2020**, *297*, 111838.
- (119) Li, H.; Yao, Y.; Zhang, J.; Du, J.; Xu, S.; Wang, C.; Zhang, D.; Tang, J.; Zhao, H.; Zhou, J. Degradation of Phenanthrene by Peroxymonosulfate Activated with Bimetallic Metal-Organic Frameworks: Kinetics, Mechanisms, and Degradation Products. *Chemical Engineering Journal* **2020**, *397* (May), 125401.
- (120) Sajjadi, S.; Khataee, A.; Bagheri, N.; Koby, M.; Şenocak, A.; Demirbas, E.; Karaoğlu, A. G. Degradation of Diazinon Pesticide Using Catalyzed Persulfate with Fe₃O₄@MOF-2 Nanocomposite under Ultrasound Irradiation. *Journal of Industrial and Engineering Chemistry* **2019**, *77*, 280–290.
- (121) Wang, L.; Jin, Q.; Xiang, Y.; Gan, L.; Xu, L.; Wu, Y.; Fang, X.; Lu, H.; Han, S.; Cui, J. Rational Design of CoxMn₃-XO₄ Embedded Carbon Composites from MOF-74 Structure for Boosted Peroxymonosulfate Activation: A Dual Pathway Mechanism. *Chemical Engineering Journal* **2022**, *435* (P2), 134877.
- (122) Li, X.; Zhang, W.; Liu, Z.; Wang, S.; Zhang, X.; Xu, B.; Yu, P.; Xu, Y.; Sun, Y. Effective Removal of Tetracycline from Water by Catalytic Peroxymonosulfate Oxidation over Co@MoS₂: Catalytic Performance and Degradation Mechanism. *Sep. Purif. Technol.* **2022**, *294* (April), 121139.
- (123) Wang, Y.; Gao, C. Y.; Zhang, Y. Z.; Leung, M. K. H.; Liu, J. W.; Huang, S. Z.; Liu, G. L.; Li, J. F.; Zhao, H. Z. Bimetal-Organic Framework Derived CoFe/NC Porous Hybrid Nanorods as High-Performance Persulfate Activators for Bisphenol A Degradation. *Chemical Engineering Journal* **2021**, *421* (P2), 127800.
- (124) Liu, M.; Liu, Y.; Liu, X.; Chu, C.; Yao, D.; Mao, S. Peroxydisulfate Activation by 2D MOF-Derived Ni/Fe₃O₄ Nanoparticles Decorated in 3D Graphene Oxide Network. *Sep. Purif. Technol.* **2022**, *301*, 121967.
- (125) Wang, J.; Wang, S. Preparation, Modification and Environmental Application of Biochar: A Review. *J. Clean Prod* **2019**, *227*, 1002–1022.
- (126) Yan, J.; Gong, L.; Chai, S.; Guo, C.; Zhang, W.; Wan, H. ZIF-67 Loaded Lotus Leaf-Derived Biochar for Efficient Peroxymonosulfate Activation for Sustained Levofloxacin Degradation. *Chem. Eng. J.* **2023**, *458*, 141456.
- (127) Zhang, Z.; Yu, Q.; Dai, Y.; Feng, B. Biochar Supported Magnetic ZIF-67 Derivatives Activated Peroxymonosulfate for the Degradation of Ciprofloxacin: Radical and Nonradical Pathways. *Colloids Surf. A Physicochem Eng. Asp* **2023**, *657* (PA), 130559.
- (128) Lei, Y.; Guo, X.; Jiang, M.; Sun, W.; He, H.; Chen, Y.; Thumavichai, K.; Ola, O.; Zhu, Y.; Wang, N. Co-ZIF Reinforced Cow Manure Biochar (CMB) as an Effective Peroxymonosulfate Activator for Degradation of Carbamazepine. *Appl. Catal., B* **2022**, *319*, 121932.

(129) Liu, J.; Jiang, J.; Wang, M.; Kang, J.; Zhang, J.; Liu, S.; Tang, Y.; Li, S. Peroxymonosulfate Activation by Cobalt Particles Embedded into Biochar for Levofloxacin Degradation: Efficiency, Stability, and Mechanism. *Sep Purif Technol.* **2022**, *294* (May), 121082.

(130) Shi, Y.; Feng, D.; Ahmad, S.; Liu, L.; Tang, J. Recent Advances in Metal-Organic Frameworks-Derived Carbon-Based Materials in Sulfate Radical-Based Advanced Oxidation Processes for Organic Pollutant Removal. *Chemical Engineering Journal* **2023**, *454* (P3), 140244.

(131) Jais, F. M.; Ibrahim, S.; Chee, C. Y.; Ismail, Z. Solvothermal Growth of the Bimetal Organic Framework (NiFe-MOF) on Sugarcane Bagasse Hydrochar for the Removal of Dye and Antibiotic. *J. Environ. Chem. Eng.* **2021**, *9* (6), 106367.

(132) Li, Y.; Hagos, F. M.; Chen, R.; Qian, H.; Mo, C.; Di, J.; Gai, X.; Yang, R.; Pan, G.; Shan, S. Rice Husk Hydrochars from Metal Chloride-Assisted Hydrothermal Carbonization as Biosorbents of Organics from Aqueous Solution. *Bioresour. Bioprocess* **2021**, *8*, 99 DOI: 10.1186/s40643-021-00451-w.

(133) Chen, X. L.; Li, F.; Zhang, M. Y.; Liu, B.; Chen, H. Y.; Wang, H. J. Highly Dispersed and Stabilized Co₃O₄/C Anchored on Porous Biochar for Bisphenol A Degradation by Sulfate Radical Advanced Oxidation Process. *Sci. Total Environ.* **2021**, *777*, 145794.

(134) Fan, Y. H.; Li, Y. Q.; Hayat, F.; Liu, C.; Li, J.; Chen, M. Multi-Targeted Removal of Coexisted Antibiotics in Water by the Synergies of Radical and Non-Radical Pathways in PMS Activation. *Sep. Purif. Technol.* **2023**, *305*, 122475.

(135) Lu, Y.; Liu, C.; Mei, C.; Sun, J.; Lee, J.; Wu, Q.; Hubbe, M. A.; Li, M. C. Recent Advances in Metal Organic Framework and Cellulose Nanomaterial Composites. *Coord. Chem. Rev.* **2022**, *461*, 214496.

(136) Kanti Chattopadhyay, P.; Ranjan Singha, N. MOF and Derived Materials as Aerogels: Structure, Property, and Performance Relations. *Coord. Chem. Rev.* **2021**, *446*, 214125.

(137) Wang, L.; Xu, H.; Gao, J.; Yao, J.; Zhang, Q. Recent Progress in Metal-Organic Frameworks-Based Hydrogels and Aerogels and Their Applications. *Coord. Chem. Rev.* **2019**, *398*, 213016.

(138) Ren, W.; Gao, J.; Lei, C.; Xie, Y.; Cai, Y.; Ni, Q.; Yao, J. Recyclable Metal-Organic Framework/Cellulose Aerogels for Activating Peroxymonosulfate to Degrade Organic Pollutants. *Chem. Eng. J.* **2018**, *349*, 766–774.

(139) Wang, X.; Zhuang, Y.; Shi, B. Degradation of Trichloroacetic Acid by MOFs-Templated CoFe/Graphene Aerogels in Peroxymonosulfate Activation. *Chemical Engineering Journal* **2022**, *450* (P2), 137799.

(140) Wu, Y.; Li, Y.; Zhao, T.; Wang, X.; Isaeva, V. I.; Kustov, L. M.; Yao, J.; Gao, J. Bimetal-Organic Framework-Derived Nanotube@cellulose Aerogels for Peroxymonosulfate (PMS) Activation. *Carbohydr. Polym.* **2022**, *296* (June), 119969.

(141) Sun, W.; Thummavichai, K.; Chen, D.; Lei, Y.; Pan, H.; Song, T.; Wang, N.; Zhu, Y. Co-Zeolitic Imidazolate Framework@cellulose Aerogels from Sugarcane Bagasse for Activating Peroxymonosulfate to Degrade p-Nitrophenol. *Polymers (Basel)* **2021**, *13* (5), 739.

(142) Wu, Y.; Ren, W.; Li, Y.; Gao, J.; Yang, X.; Yao, J. Zeolitic Imidazolate Framework-67@Cellulose Aerogel for Rapid and Efficient Degradation of Organic Pollutants. *J. Solid State Chem.* **2020**, *291* (July), 121621.

(143) Cao, J.; Yang, Z.; Xiong, W.; Zhou, Y.; Wu, Y.; Jia, M.; Peng, H.; Yuan, Y.; Xiang, Y.; Zhou, C. Three-Dimensional MOF-Derived Hierarchically Porous Aerogels Activate Peroxymonosulfate for Efficient Organic Pollutants Removal. *Chem. Eng. J.* **2022**, *427*, 130830.

(144) Chen, M. M.; Niu, H. Y.; Niu, C. G.; Guo, H.; Liang, S.; Yang, Y. Y. Metal-Organic Framework-Derived CuCo/Carbon as an Efficient Magnetic Heterogeneous Catalyst for Persulfate Activation and Ciprofloxacin Degradation. *J. Hazard Mater.* **2022**, *424* (PA), 127196.